

## Reply to C. Kuehn

Mark S. Williamson<sup>1</sup>, Sebastian Bathiany<sup>2</sup>, and Timothy M. Lenton<sup>1</sup>

<sup>1</sup>Earth System Science group, College of Life and Environmental Sciences, University of Exeter,  
Laver Building, North Park Road, Exeter EX4 4QE, UK

<sup>2</sup>Aquatic Ecology and Water Quality Management, Wageningen University, PO Box 47,  
Wageningen, Netherlands

Correspondence to: Mark S. Williamson (m.s.williamson@exeter.ac.uk)

We would like to thank the referee for his detailed and thoughtful comments on our manuscript.  
We reply below (the referee's original text in italics followed by our response):

5 *My suggestions for the authors would be to take the paper into one of two possible  
directions for a major revision. Either, (I) one does incorporate and compare a lot more  
to available techniques and previous results on time-periodic dynamical systems. How-  
ever, this does seem to be out of the focus of ESD a bit. A second alternative (II) would  
be to shorten the mathematical part and clearly identify some of the warning signs as  
the same ones as if one would use return-map methods. With the now available space  
one could either try to apply techniques to other forced climate models and draw ap-  
plied conclusions, or look at more time series. These are the stronger parts of this paper  
10 and probably more adequate for ESD anyhow. Either way, some re-writing is necessary  
to embed the problem in a more proper way into previously developed and available  
techniques. Overall, I think if the authors should pursue a major revision using the sec-  
ond option (II), then I could see the revised paper to be a very solid contribution to  
15 ESD.*

We also agree the second alternative would be the best way to take a revised manuscript and  
this is the direction we have broadly taken in line with the referee's recommendations. We have  
added discussions of existing techniques and previous literature into the introduction of the revised  
manuscript including the return map method which we have applied to the examples in the previ-  
20 ous manuscript which we agree was lacking from the original. It turns out the return map method  
is complementary to the phase lag and response amplification in that in one regime one set of in-  
dicators is not useful while the other is. The systems we were largely concerned with in this and  
the previous manuscript are best handled with phase lag and response amplification which was the  
reason we did not use return maps in the original manuscript. We discuss this further in the reply  
25 to the referee's point (1). We have also extensively restructured the manuscript and included sliding  
window analysis of harmonic amplitude increasing on approach of a local bifurcation (a suggestion

of referee #2). Although the manuscript has a slightly revised title, many new figures and has been significantly restructured to include a more thorough discussion, the technical content, main points and conclusions are unchanged from the previous manuscript although they are strengthened.

30 We would have liked to apply our method to more examples in the Earth system but feel the paper is coherent with an expanded analysis of Arctic sea ice. Plenty of components of the climate are periodically forced for example by the solar insolation and have similar time scales to this forcing, however we could not think of any that are conjectured to be approaching a local bifurcation apart from the Arctic sea ice.

35 We did consider including analysis of a simple vegetation-savannah model which had a local bifurcation due to variations in precipitation. We decided not to include this as the model was a bit simplified and added nothing new to the manuscript, being very similar to the double well example.

*However, as far as I can see from the paper, the authors also claim that their methods and mathematical ideas for early-warning signs are novel. At least, the bulk of the paper*  
40 *is dedicated to this topic and they use "here we find..." and "we show that..." and similar formulations to indicate that their approach is new. In my opinion, the major problem I see with this work is that the authors did not seem to make enough of an effort to link and/or base their results on previously available mathematical techniques. I will give the authors the benefit of the doubt that they simply did not know, or could not find the*  
45 *adequate sources on which their analysis could have been based and/or compared to since it may not be in the climate-science related journals (and it could very well be common to just argue things are novel if they have not appeared in a certain subsets of journals; in general, this is a view which I disagree with, particularly for such a highly interdisciplinary topic as nonlinear dynamics).*

50 The mathematics we use in the manuscript are very simple and clearly not novel. So much so in fact that it becomes hard to cite a relevant source as any student of physics or engineering will very likely have solved the equation for the damped harmonic oscillator forced periodically and found the solution in the overdamped limit has a phase lag and an amplitude depending on the damping parameter. For instance one can look in any undergraduate level text on oscillations and waves and  
55 find these solutions. We have cited one such example in the revised manuscript and a discussion of this point. However, we have not been able to find any other authors using the phase lag, amplification response and increase in harmonic amplitude as an indicator of the approach of a local bifurcation. Of course, we would not be surprised if this was not the case since the method is very simple, which is the reason incidently, that we like it! Because of this simplicity, we have been careful not to make  
60 novelty claims in the previous manuscript but we have eliminated the offending 'we show' in the revised version.

65 1) For periodic systems, there is a well-developed theory of return maps which converts the continuous-time periodic orbit into questions about the local fixed point of a return map (see e.g. the books by Kuznetsov or Guckenheimer/Holmes or in fact many other dynamical systems texts). It is really strange that the authors do not even mention this approach to the problem. A very natural approach would be to just to try to re-use results about slowing down and early-warning signs for local bifurcations for periodic systems by looking at a return map. Of course, the change of the lag will not be visible directly in the return map, so it would be reasonable to try to do a comparison why 70 in certain circumstances the lag might be a better or worse warning sign compared to quantities computed directly from the return map.

We agree we should have mentioned the return map method and this is indeed another way of looking for early warning signals of local bifurcations. The motivation for the method outlined in the manuscript was that we were looking at the particular case of the conjectured Arctic sea ice 75 bifurcation and for this system the forcing (the annual cycle of insolation) is about the same order as the time scale of the sea ice (order of months, possibly a couple of years).

Recall methods used for looking for local bifurcations are based on detecting a decrease in the stability of the system's steady state by inferring the change in time taken for perturbations away from that steady state to decay. If the steady state is a fixed point, one usually thinks of the noise 80 in the system as the perturbation and infers the system time scale by sampling the system's state at some time interval and computing the correlation between successive time intervals resulting from the perturbation's decay. If the steady state is periodic, like the ones considered in this manuscript, one approach is to sample the system once every cycle to obtain a new time series that can be treated as a fixed point steady state, but now the interval between samples of the system state has increased. 85 This is the return map method and one can repeat the fixed point, compute correlations between the now increased, successive time intervals.

For the cases we consider in the manuscript, where the period of the forcing is of the same order as the time scale of the system such as the sea-ice, the return map would take an annual time series with the resolution of a day if desired (essentially a continuous flow) and convert it to a single point 90 per cycle, that is one data point per year (a discrete map),  $T$ . There are two problems with this: (i) there are far less data points to analyze in the time series so any trend in the signal becomes harder to detect with statistical indicators as the standard error scales  $1/\sqrt{N}$  ( $N$  is number of data points in the time series) and (ii) more importantly, even if there was critical slowing down, since the time scale of the system,  $\tau$  may be smaller or of the same order of the resolution of the return map time series, detection becomes very difficult or impossible i.e. the time taken for a perturbation to decay 95 back to the steady state is less than the interval between data points resulting in little or no correlation between the data points in the return map. One also cannot reliably use autocorrelation, the usual

indicator of noisy slowing down of fixed points, to infer time scale as an assumption in the derivation is that  $T/\tau$  is small which it is not in this case.

100 In addition, for the case of the sea-ice, the opportunity of having such an easy to spot, deterministic system response to the annual forcing (which one can think of as a very predictable perturbation) to exploit to infer system time scale without having to do any detailed manipulation of the data motivated our approach.

We therefore realized very early on in the investigation that a return map method would very likely  
105 not be useful and is not useful for the cases the phase lag and response amplification are most useful. This gave the resulting 'ignore-return-map-tunnel-vision' in the manuscript which on reflection we should have reviewed and critiqued. We have rectified this in the revised manuscript. The cases where the phase lag and response amplification work well ( $\omega\tau \sim 1$ ) are not well suited to return map analysis. Conversely when the interval between return map data points is smaller than the system  
110 time scale,  $\tau/T \geq 1$  (equivalent to  $\omega\tau \geq 2\pi$ ), a reasonable condition for return map analysis to work well, phase lag and response amplification tend to asymptote and are not so useful. The two methods therefore have some complementarity.

We have included figures illustrating this complementarity in the revised manuscript. Figure 1 is essentially the same as figure 2 in our manuscript except we have varied  $D_m$  over 100 cycles instead  
115 of 25. This is because we need extra data points to calculate the autocorrelation of the return maps with any reliability. We have also added Gaussian white noise to  $\dot{x}$  of standard deviation 0.01 as the return map method needs small perturbations to work. In figure 2 we have plotted all the early warning indicators for this system including the return map calculated with a sliding window of 25 cycles. The black lines are the theoretical curves and the coloured lines are the estimated curves. The  
120 key point is the theory and estimated autocorrelations do not show anything in this regime ( $\omega\tau \sim 1$ ). In figures 3 and 4 we have plotted the same quantities but with decreased period of forcing ( $T = 1/4$  so  $\omega\tau \sim 4\pi$ ). This is a regime in which phase lag and response amplitude start to asymptote and are therefore not so useful to infer changing system time scale. However, autocorrelation of the return map now becomes useful as can be seen in the figure. This system is going in the  $\omega\tau \gg 1$  regime  
125 which we have previously discussed in the manuscript.

From the sea-ice time scale of 6 months estimated using phase lag ( $\omega\tau \sim \pi$ ) we did not expect the return map method to be useful. However, these estimates are uncertain so we also calculated the return map for completeness. The results confirm return map analysis is not useful for this case. Specifically we show autocorrelation in a sliding window of the return map time series is very un-  
130 certain and/or small.

We have added discussion of these points in similar or more detail in the revised manuscript.

*2) The authors are also apparently not aware that there is already quite a bit of very classical work on early-warning signs for periodic systems. For example, it should be mentioned that warning signs for bifurcations have already appeared for periodic orbits*

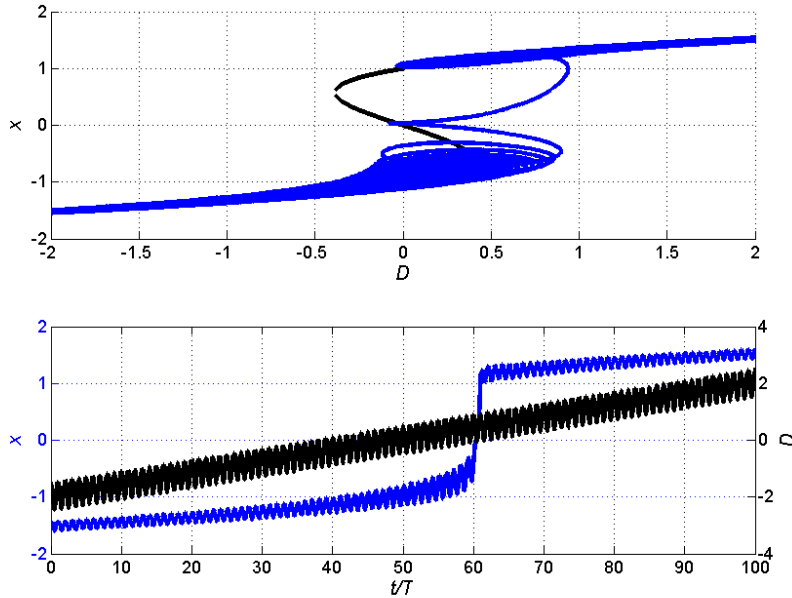


**Figure 1.**  $\omega\tau \sim 1$ : Same figure as figure 3 in the manuscript except variation of  $D_m$  is over more cycles to generate more points for a reliable return map analysis and weak Gaussian white noise of standard deviation 0.01 is added. Parameters are set to  $D_a = 1/2$ ,  $T = \pi$  (the same order as the system time scale  $\tau$ ) and  $D_m$  is varied linearly with time between -2 and 2 over about 100 cycles. In the upper panel the black lines are the nullclines while the system response is the blue line plotted against  $D(t)$ . In the lower panel we have plotted the system response (blue) against the forcing  $D$  against  $t/T$ .

135      *many years ago in the groundbreaking work by Wiesenfeld: Wiesenfeld, K. (1985). Noisy precursors of nonlinear instabilities. Journal of Statistical Physics, 38(5-6), 1071-1097. Furthermore, there is also a lot of recent activity on the field as exemplified by the recent work: Zhu, J., Kuske, R., and Erneux, T. (2014). Tipping points near a delayed saddle node bifurcation with periodic forcing. arXiv preprint arXiv:1410.5101. I am pretty sure*

140      *that upon further search one would be able to come up with a rather long list of papers that have studied periodic orbits near instability and their statistical, Fourier-analysis, and phase properties. Then it is a natural question which of these results can be applied directly to the problem of early-warning signs. The authors simply skip this step in their analysis. There is one mention to stochastic resonance, and also in this part of the*

145      *literature I would expect to find already a lot of readily applicable results. Of course, after this detailed review, one could try to do a direct and/or different calculation, do a comparison and then argue which parts are new/old, better/worse, etc.*

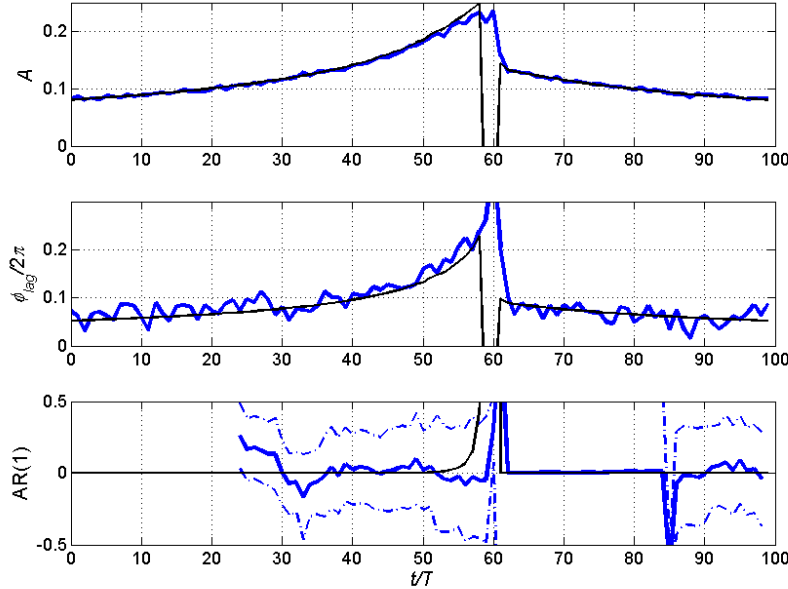


**Figure 2.**  $\omega\tau \sim 1$ : The early warning indicators, response amplification (upper panel),  $A = \frac{D_a\tau}{\sqrt{1+\omega^2\tau^2}}$ , and phase lag (middle panel),  $\frac{\phi_{lag}}{2\pi} = \frac{1}{2\pi} \arctan(\omega\tau)$  calculated for the time series in figure 1. In the lower panel, autocorrelation of a sliding window of 25 points of the return map is plotted with standard errors on the estimate. Black lines are theoretical curves of all the quantities. Phase lag and amplitude response are useful quantities here however the return map is not.

We have added more context and review of previous literature in a revised manuscript, some quoted directly below:

150 'Abrupt change in a system can occur due to a bifurcation - that is, a small smooth change in parameter values can result in a sudden or topological change in the system's attractors. Extreme sensitivity of systems close to criticality is familiar from studies of critical phenomena in statistical mechanics Domb et al. (1972-2001) and stability analysis in nonlinear dynamical systems Kuznetsov (2004).'

155 We have also briefly reviewed Wiesenfeld's work and mentioned how it differs from ours:

'In an elegant study Wiesenfeld (1985) computed the Fourier spectra of noisy perturbations in systems with periodic attractors. Very close to a local bifurcation, the dominant system time scale asymptotes towards infinity causing the dynamics of the noisy perturbations away from the attractor to be dependent only on the type of bifurcation and not on the details of the system's specific equations. This observation allowed the author to classify all codimension 1 bifurcations in an arbitrary periodic system by the harmonics in the spectra of residuals. He called these early warning signals noisy precursors.'

160

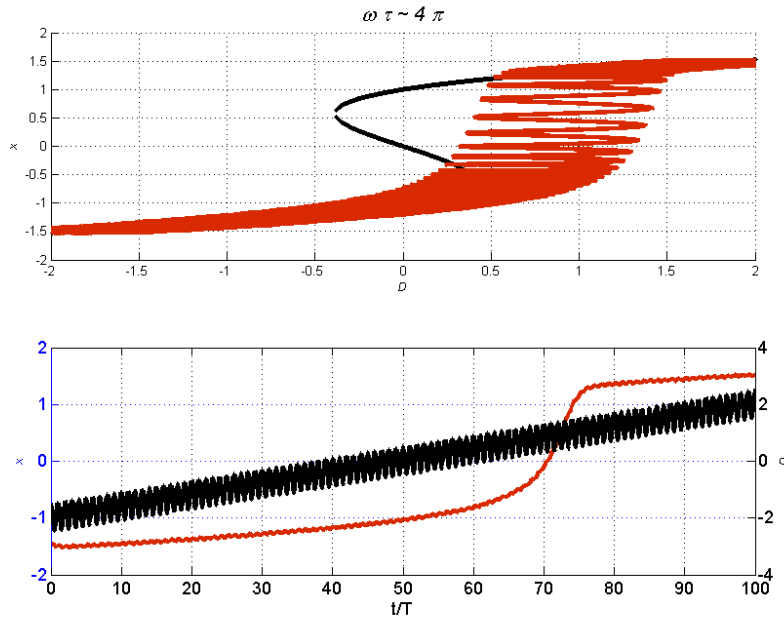


**Figure 3.**  $\omega \tau \sim 4 \pi$ : Same figure as figure 1 except the period of forcing is decreased to  $T = 1/4$ . Parameters are set to  $D_a = 1/2$  and  $D_m$  is varied linearly with time between -2 and 2 over about 100 cycles. In the upper panel the black lines are the nullclines while the system response is the blue line plotted against  $D(t)$ . In the lower panel we have plotted the system response (blue) against the forcing  $D$  against  $t/T$ .

And when describing using the harmonics in the response:

‘With a similar motivation Wiesenfeld (1985) and Wiesenfeld and McNamara (1986) calculated the Fourier spectra of the perturbations, rather than the response, away from periodic attractors very close to local bifurcations with noisy and weak periodic modulation respectively.’

We have mentioned work on stochastic resonance where appropriate. The simplest systems this community studies are essentially our conceptual model, that is a periodically driven double well potential, but with the added complication of additive Gaussian noise. They have studied phase response, amplitude and Fourier spectra in this context. However, they are interested in hopping between the wells with some barrier height (the ‘stochastic resonance’) rather than bifurcations (barrier height goes to zero) as in our study.

The other reference the referee mentions, Zhu et al. (2015), seems of limited relevance. These authors look at the well known phenomenon of delayed bifurcation when the control parameter is slowly varied compared to the static case. The control parameter in their study, instead of linearly increasing with time is now periodic with changes in amplitude and frequency. At the end of the paper they use a simple sea ice model as an example of this. We have therefore chosen not to include this work.

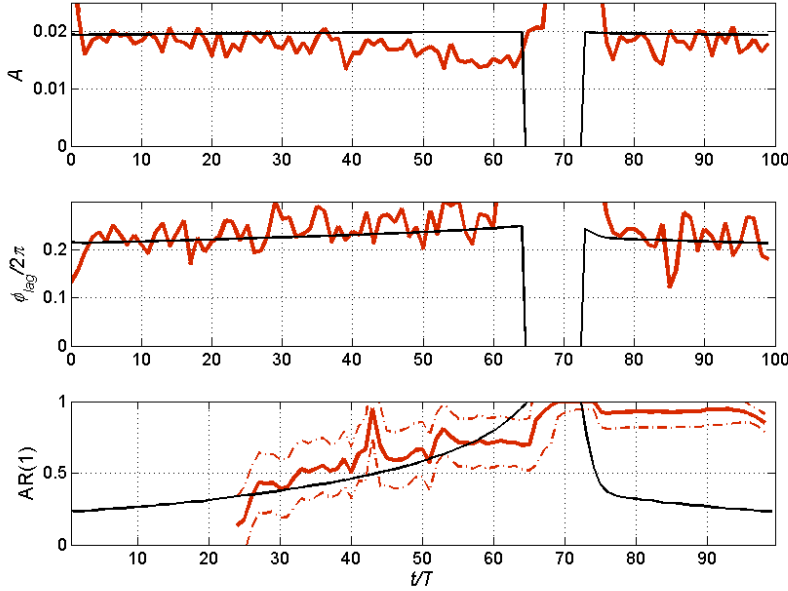


**Figure 4.**  $\omega\tau \sim 4\pi$ : The early warning indicators, response amplification (upper panel),  $A = \frac{D_a\tau}{\sqrt{1+\omega^2\tau^2}}$ , and phase lag (middle panel),  $\frac{\phi_{lag}}{2\pi} = \frac{1}{2\pi} \arctan(\omega\tau)$  calculated for the time series in figure 3. In the lower panel, autocorrelation of a sliding window of 25 points of the return map is plotted with standard errors on the estimate. Black lines are theoretical curves of all the quantities. Phase lag and amplitude response have now asymptoted and are not useful quantities however the return map now becomes useful.

180 3) Since the authors deal with a time-dependent non-autonomous system when using the variational equation around the periodic orbit before averaging out to a mean value, it is also very natural to ask which classical results from Floquet theory and non-autonomous dynamical systems could be applied for finding early-warning signs for tipping points. In this context, there are many different notions for a spectrum if we go beyond classical Floquet theory. For example, what about looking at finite-time  
 185 Lyapunov exponents, the dichotomy spectrum, etc and simply see what these quantities say as warning signs? At least, things like FTLEs are easily computable via standard packages so there really is very little effort involved in doing these calculations and comparing it to the direct calculations the authors do. I would even guess that from return map data, return times and FTLEs, one should be able to recover identical or very  
 190 similar warning signs...

These ideas may be potentially useful lines of future investigation. However, we are not familiar with all the techniques the referee mentions or how they could be applied to time series analysis in climate applications where the dynamical equations are not known and one's control on the system



for repeatable experiments is limited or non-existent. We would be interested to hear the referee's  
195 opinion on this.

Although we are interested to hear more about this, the comment is more in line with the first,  
rather than the referee recommended and author chosen second direction to take a revised manuscript.

4) *The authors also spend a long part of the paper on discussing the issue of time  
scales and relevant limits. This issue has been discussed in a very analogous situa-  
200 tion regarding noise-induced and bifurcation-induced transitions. Depending upon the  
time scale of the noise relative to the parameter drift one either sees noise-induced or  
bifurcation-induced transitions in certain classes of systems. See for example: Ashwin,  
P., Wieczorek, S., Vitolo, R., and Cox, P. (2012). Tipping points in open systems: bifurca-  
tion, noise-induced and rate-dependent examples in the climate system. Philosophical  
205 Transactions of the Royal Society of London A: Mathematical, Physical and Engineer-  
ing Sciences, 370(1962), 1166-1184. Kuehn, C. (2013). A mathematical framework for  
critical transitions: normal forms, variance and applications. Journal of Nonlinear Sci-  
ence, 23(3), 457-510. In fact, the issue has appeared in many works implicitly before  
these works in stochastic multiscale systems. Here the situation is very similar except  
210 that there is now instead of the noise-focus a comparison between the forcing scale and  
parameter drift scale. Therefore, it is actually quite easy to see that there should be two  
asymptotic regimes and one intermediate regime as for the noise/parameter case also in  
the forcing/parameter case. In fact, noise terms are frequently just be treated as forcing  
terms if the noise is smooth enough and maybe one could even transfer previous results  
215 via this view.*

We are in agreement with the referee. This is the central issue in applying early warning techniques  
and this is why we spend some time discussing it.

## References

- Domb, C., Green, M. S., and Lebowitz, J., eds.: Phase transitions and critical phenomena, vol. 1-20, Academic  
220 Press, 1972-2001.
- Kuznetsov, Y. A.: Elements of Applied Bifurcation Theory, third edition, Springer, 2004.
- Wiesenfeld, K.: Noisy precursors of nonlinear instabilities, *J. Stat. Phys.*, 38, 1071–1097, 1985.
- Wiesenfeld, K. and McNamara, B.: Small-signal amplification in bifurcating dynamical systems, *Phys. Rev. A*,  
33, 629–641, 1986.
- 225 Zhu, J., Kuske, R., and Erneux, T.: Tipping points near a delayed saddle node bifurcation with periodic forcing,  
arXiv:1410.5101v2, 2015.

## Reply to Anonymous referee #2

Mark S. Williamson<sup>1</sup>, Sebastian Bathiany<sup>2</sup>, and Timothy M. Lenton<sup>1</sup>

<sup>1</sup>Earth System Science group, College of Life and Environmental Sciences, University of Exeter,  
Laver Building, North Park Road, Exeter EX4 4QE, UK

<sup>2</sup>Aquatic Ecology and Water Quality Management, Wageningen University, PO Box 47,  
Wageningen, Netherlands

Correspondence to: Mark S. Williamson (m.s.williamson@exeter.ac.uk)

We thank the referee for their time and generally positive appraisal of our manuscript. Many of the concerns of referee 2 are the same as our first referee and our responses to these concerns, if not detailed enough below, can be found in our reply to Christian Kuehn. We reply below (ref #2's original text in italics followed by our response):

5            *In my opinion, the main issue is that the proposed mathematical techniques are not  
novel (as already pointed out by Reviewer 1) although they are presented as such. It is  
really strange that the manuscript completely disregards previous work in the literature  
in this area. There is the pioneering work by Wiesenfeld (Journal of Statistical Physics,  
1985). It appeared long before the subject of critical transitions became so popular in  
10            the applied sciences and the buzz word of a "tipping point" was even created. There is  
the recent study by Zhu, Kuske and Erneux (2014) which goes in a similar direction as  
the authors' work. Reviewer 1 is pointing out more previously developed techniques the  
present work should be linked to.*

We agree that we should have referenced previous work more thoroughly and this has been recti-  
15            fied in a revised version of the manuscript. Please see our first response to Christian Kuehn and his  
point (1) and (2) for more details.

*Maybe the authors should present more applications of their techniques to earth  
system components rather than just mentioning possible candidates.*

Please see our first response to Christian Kuehn.

20            *Figure 8 just shows that the annual cycle in the Arctic sea ice area data is quite  
strongly aharmonic, corresponding to a nonlinear response of the system to the solar  
insolation forcing, as is well known and already clearly visible by eye from the time  
series. The evolution of the strength of the nonlinearity over time, which is actually  
proposed by the authors as an early-warning signal when approaching a possible bifur-  
25            cation, is not considered at all.*

This is a good point and we thank the referee for pointing this out. We assumed mistakenly that to reliably resolve the peaks of the harmonics in the Fourier spectra would require a large amount of data that would make a sliding window analysis of the time series difficult. It turns out for the Arctic sea-ice observations one can reliably resolve the peaks with only 10 full cycles. We have therefore  
30 been able to plot harmonic amplitude against time using a sliding window of 10 years and have added this analysis. Like the other indicators for the sea ice, no convincing trend is seen. We have also included the same analysis for the conceptual model example showing the harmonic amplitudes increasing as the local bifurcation is approached.

## **Changes in the revised manuscript**

The changes made in the revised manuscript are extensive but are in line with the referee recommendations. We have

- Added previous literature for context and how it differs with work in the revised manuscript. Specifically in the introduction and sections 2 and 3.
- Restructured manuscript to include return map analysis and review. Specifically we have combined section 3 and section 4 and moved them to section 2. The new section 2 has a discussion of return maps. The new section 3 is a combination of old sections 2 and most of section 5. The new section 4 is old section 5B.
- Included new figures to show the complementarity between return maps and phase lag in different time scale regimes.
- Included new figures of harmonic amplitude evolution.

Please note that the technical content and conclusions remain unchanged. Only material relating to return maps has been added. Previous literature and context has also been added.

# Early warning signals of tipping points in periodically forced systems

Mark S. Williamson<sup>1</sup>, Sebastian Bathiany<sup>2</sup>, and Timothy M. Lenton<sup>1</sup>

<sup>1</sup>Earth System Science group, College of Life and Environmental Sciences, University of Exeter, Laver Building, North Park Road, Exeter EX4 4QE, UK

<sup>2</sup>Aquatic Ecology and Water Quality Management, Wageningen University, PO Box 47, Wageningen, Netherlands

Correspondence to: Mark S. Williamson (m.s.williamson@exeter.ac.uk)

**Abstract.** The prospect of finding generic early warning signals of an approaching tipping point in a complex system has generated much recent interest. Existing methods are predicated on a separation of timescales between the system studied and its forcing. However, many systems, including several candidate tipping elements in the climate system, are forced periodically at a timescale comparable to their internal dynamics. Here we ~~find~~use alternative early warning signals of tipping points due to local bifurcations in systems subjected to periodic forcing whose time scale is similar to the period of the forcing. These systems are not in, or close to, a fixed point. Instead their steady state is described by a periodic attractor. ~~We show that the~~ For these systems, phase lag and amplification of the system response can provide early warning signals, based on a linear dynamics approximation. Furthermore, the ~~power~~Fourier spectrum of the system's time series reveals ~~the generation of~~ harmonics of the forcing period ~~, the size of which are proportional in the system response whose amplitude is related~~ to how nonlinear the system's response is becoming with nonlinear effects becoming more prominent closer to a bifurcation. We apply these indicators as well as a return map analysis to a simple conceptual system and satellite observations of Arctic sea ice area, the latter conjectured to have a bifurcation type tipping point. We find no detectable signal of the Arctic sea ice approaching a local bifurcation.

## 1 Introduction

The potential for early warning of an approaching abrupt change or 'tipping point' in a complex, dynamical system has been the focus of much ~~recent~~ research, see for example ~~Scheffer et al. (2009); Lenton (2011); Wiesenfeld (1985), Held and Kleinen (2004), Thompson and Sieber (2011)~~ and Scheffer et al. (2012). Abrupt change in a system can occur due to a bifurcation - that is, a small smooth change in parameter values can result in a sudden or topological change in the system's attractors. This extreme sensitivity of systems close to criticality is familiar from studies of critical phenomena in statistical mechanics (Domb et al. (1972-2001)) and stability analysis in nonlinear dynamical

25 systems (Kuznetsov (2004)). Much work on the anticipation of bifurcations from time series data ~~;~~  
e.g. in ecosystems (~~Scheffer et al. (2009)~~Carpenter et al. (2011)), or the climate system (Dakos et al.  
(2008) and Lenton (2011)), ~~has been based on~~ is based on methods that infer the time taken for the  
system to recover to its steady state (the system's time scale) from perturbations away from that  
steady state. The methods are usually based on a clear separation of three time scales: (i) The time  
30 scale of the dynamics of the system one wants to study, (ii) much faster processes than the time scale  
of the system, usually thought of as the perturbations the system recovers from and (iii) much slower  
processes than the time scale of the system which govern the present system steady state. In addition,  
the system dynamics are modelled as overdamped, the fast dynamics as a noisy, normally distributed  
random variable of small variance and the slow dynamics as a constant, control parameter ~~on the time~~  
35 ~~scale of the system~~. Provided these are good working approximations, critical slowing down ~~;~~ the  
increase of the system's time scale, is expected prior to a local bifurcation and can be detected by  
computing the ~~autocorrelation~~ lag 1 autocorrelation in a sliding window of a system's time series. An  
increasing trend in autocorrelation ~~in time~~ shows the stability of the system is weakening or equiv-  
alently, the system's time scale is increasing - which is a generic feature of a system approaching a  
40 local bifurcation. Provided the variance of the fast noisy process is constant, increasing variance of  
the system's time series is also a good indicator of critical slowing down, although it is less robust  
than lag 1 autocorrelation due to its dependence on the noisy process.

For many systems of interest one or more of the above assumptions may be invalid (Williamson and Lenton (2015)).  
In particular, when the forcing of a system has a comparable period to the time scale of the system,  
45 the forcing cannot be modelled as a slow, constant control parameter or a fast, random process. ~~Here~~  
~~we give alternative early warnings signals of approaching local bifurcations when the period of the~~  
~~forcing is similar to the time scale of the system. Systems of this type,~~ however they can still be  
thought of as a perturbation away from the system steady state that one can measure the recovery  
time from, an observation we exploit in this manuscript. These systems are particularly relevant in  
50 the climate system where periodic forcing is a consequence of the motion of the Earth relative to the  
Sun. For example, solar insolation variation from the diurnal, annual or Milankovich cycles. These  
systems have steady states described by periodic attractors rather than the simpler, fixed point type  
attractors required for lag 1 autocorrelation and variance to be used as early warning indicators.

In an elegant study Wiesenfeld (1985) computed the Fourier spectra of noisy perturbations in  
55 systems with periodic attractors. Very close to a local bifurcation, the dominant system time scale  
asymptotes towards infinity causing the dynamics of the noisy perturbations away from the attractor  
to be dependent only on the type of bifurcation and not on the details of the system's specific  
equations. This observation allowed the author to classify all codimension 1 bifurcations in an  
arbitrary periodic system by the harmonics in the spectra of residuals. He called these early warning  
60 signals noisy precursors.

A common method to study stability changes in periodic attractors is the return or Poincaré map, see Strogatz (2001). Here, one converts the continuous-time periodic orbit into the fixed point of a return map by sampling the orbit once every period. One can then compute the usual fixed point indicators for the resulting return map time series such as lag 1 autocorrelation and variance. Advantages of this approach include no linearity requirement on the dynamics of the periodic attractor although perturbations away from the attractor must be small enough to be treated linearly. One can also handle systems with internally generated cycles rather than those generated by external periodic forcing that we look at in this manuscript. To detect any change in stability from the return map the time scale of the system must also be greater than the period of the forcing. To see this, imagine one samples the cycle to create a point in the return map and then immediately after perturbs the system away from the stable cycle. If the system time scale is shorter than the cycle period, which is determined by the forcing period, the system will have recovered back to the stable cycle before the system is sampled again for the next point in the return map. The perturbation and its recovery will therefore be invisible to stability analysis on the return map time series. It should be noted that close to a local bifurcation the system time scale approaches infinity so satisfying this requirement. However, if this requirement is met only over a few cycles or less it will be very hard to detect.

With this limitation in mind we suggest alternative early warnings signals of approaching local bifurcations when the period of the forcing is similar to the time scale of the system. We look particularly at sinusoidal forcing since this approximates the variation of solar insolation well. However, the method works for any periodic forcing and we also give the derivation of the general case in the appendix.

~~We show~~ We demonstrate that increasing system time scale as it approaches a local bifurcation shows up as an increasing phase lag in the system response relative to the forcing. In addition, we show the amplitude of the system response increases as well. These indicators, like lag 1 autocorrelation and variance in ~~the usual method~~ fixed point attractor methods, assume the linearized dynamics approximate the true nonlinear dynamics well. One might ask how well the linear approximation works, especially near the bifurcation, since bifurcations are strictly nonlinear phenomena. We show how to give a quantitative answer to this question can be provided by computing the ~~power~~ Fourier spectrum of the system's time series. In particular, as the system's behaviour becomes more nonlinear, harmonics of the forcing period are generated in the system response and their amplitudes may be obtained from the system's ~~power~~ Fourier spectra. Since the system response becomes more nonlinear as one approaches the bifurcation, one can view the increasing amplitude of harmonics as another early warning signal.

The paper is organised as follows: In section ~~3 we introduce a conceptual model to illustrate periodically forced overdamped systems approaching a local bifurcation and the time scale separation problem. Then in section 2 we show that the~~ 2 the early warning indicators used in the manuscript are introduced, namely the system response phase lag and amplification ~~are good early warnings of~~



approaching local bifurcations. These indicators, like previous ones, are based on a linear dynamics approximation, however in section 2.1 we give another useful tool that allows one to quantify how good an approximation the linearized dynamics is as well as how nonlinear the system is behaving as well as harmonic amplitudes. We also review a common approach to periodic attractors, the return map, which is complementary to phase lag and response amplification. In section 3 a periodically forced overdamped system in a double well potential is used to illustrate the time scale separation problem and the properties of the early warning indicators when a local bifurcation is approached. In section ?? we calculate these indicators for a conceptual model driven towards a local bifurcation and for satellite time series data. 4 we apply the early warning indicators to satellite observations of Arctic sea ice area, a system conjectured to be approaching a local bifurcation, before concluding. We conclude in section 5.

## 2 Periodically driven fold as an idealised example

Here we use an idealized example of a periodically forced, overdamped system tipping due to

### 2 Early warning indicators of local bifurcations in periodic systems

As previously mentioned in the introduction, the Arctic sea-ice has been conjectured to be approaching a local bifurcation to illustrate time scale separation between the forcing and the system's internal time scale. We first introduce our system which has one dynamical variable,  $x$ , (see Shneidman et al. (1994); Jung and Hänggi (1993) for work on periodically driven, noisy double well systems).  $x$  evolves according to

$$\dot{x} = x - x^3 + D(t)$$

where overdots denote differentiation with respect to time,  $t$  and the periodic forcing function  $D(t)$  is

$$D(t) = D_m + D_a \cos(\omega t).$$

$D_m$  and  $D_a$  are constants and  $\omega = \frac{2\pi}{T}$  is the angular frequency and  $T$  is the period. Treating this system approximately, one can think crudely of the slow control parameter as the decrease of outgoing long-wave radiation, giving a warming trend in air temperature as the Earth's atmospheric CO<sub>2</sub> concentration increases. This is a system that is forced periodically and deterministically by the annual cycle of short-wave solar insolation. The system response is dominated by this periodic forcing rather than small amplitude, random noisy forcing also present and system time scale is roughly the same order of the forcing period. In this section, motivated by detection of local bifurcations in systems like the sea-ice type from time series, we look for suitable methods. Although this system has no clear separation of time scales with which to use fixed point methods directly, the fact that this

130 ~~system has a large and predictable perturbation one can measure the response to reduces the need for the statistical methods (and therefore large numbers of data) required for noisy perturbations and so number of data in a time series becomes less of an issue. Equation 11 models a nonautonomous nonlinear system, the overdamped limit of a Duffing oscillator (Thompson and Stewart (2002)). When there is no periodic, just constant forcing ( $\omega = 0$ ) the familiar, well studied autonomous fold bifurcation is recovered (for example see Strogatz (2001)). For  $\omega = 0$ , the solutions of  $\dot{x} = 0$ , give the system's fixed points,  $x^*$  (the nullclines) and number either one or three depending on the value of  $D_m$ . One can evaluate the stability of these fixed points by looking at the linearized dynamics close to~~

140 ~~Students of physics or engineering will likely have solved the equation for the forced damped harmonic oscillator and observed in the overdamped limit that the fixed points,  $J(x^*)$~~

$$J(x^*) = \frac{\partial \dot{x}}{\partial x} \Big|_{x=x^*} = 1 - 3x^{*2}$$

~~If  $J(x^*)$  is negative, the fixed point is stable, if it is positive it is unstable. In the region where three fixed points exist one finds two are stable and one is unstable. That is, it is a bistable region. The bistable region has boundaries marked by the local bifurcations and these can be found by solving  $J(x^*) = 0$  for  $x^*$  i.e. when the fixed point becomes neutrally stable. One can also calculate the e-folding time scale of the system in state  $x$ ,  $\tau$  from the Jacobian  $\tau = -1/J(x)$ . We will refer to the e-folding time as the system time scale. Early warning indicators are simply functions of  $J(x^*)$  or equivalently  $\tau$  phase and amplitude depend on the damping parameter (see for example Main (1993)). In the following subsections we propose to use this fact and phase lag and response amplification as simple non-statistical indicators of system time scale. We demonstrate their properties and their functional dependence on system time scale. These early warnings are based on a linear dynamics approximation but by taking the Fourier transform of the system response, one can also look the magnitude of the nonlinear response. This has two purposes, first one can check the linear approximation is good and second, because bifurcations are strictly nonlinear phenomena, the system response will become more nonlinear as one approaches the bifurcation giving another early warning indicator that can be monitored.~~

150 ~~The systems we concentrate on in this manuscript, relevant to externally forced climate problems, have cycle periods determined by the period of forcing and a one-way coupling from the forcing to the system and so are special cases of periodic attractors. For these special cases, when forcing period and system time scale are similar, phase lag and response amplification are useful indicators. However, return maps are generally more useful when treating more general periodic attractors. At the end of the section we briefly review the method of return maps.~~

## 2.1 ~~Period of forcing much slower than system time scale, $\omega\tau \ll 1$~~

Now consider how the system can be described for the asymptotics of the forcing frequency  $\omega$ .

165 First imagine that we force the system periodically, but very slowly. That is  $T \gg \tau$  and look at the behaviour of the system. Since  $D(t)$  is varying much slower than the system can respond, the system can adjust to the changing  $D(t)$  very quickly and effectively remains at a fixed point. We can therefore model  $D(t)$  as a slow constant, control parameter and all the usual assumptions (listed in the introduction) apply. In this case we can use the autocorrelation as a good early warning indicator  
170 of an approaching local bifurcation. The system state  $x$  is plotted against  $D$  and against  $t$  as the red line in figure 1.

## 2.1 Phase lag and response amplification.

### 2.2 ~~Period of forcing much faster than system time scale, $\omega\tau \gg 1$~~

The forcing is changing much faster than the system can respond to it. The forcing is so fast relative  
175 to how quickly the system can respond, the system effectively looks static and all the dynamics come from the forcing directly. In this case we can place  $D(t)$  in the fast dynamics. However, not all of the other assumptions are satisfied. It is true that  $D(t)$  is independent of  $x$ , however it is not uncorrelated with itself at different times and therefore cannot strictly be modelled as a normally distributed random variable, although at first glance it looks as though it is again possible to use the  
180 usual early warning techniques. The system state  $x$  is plotted against  $D$  and against  $t$  as the green line in figure 1.

### 2.2 ~~Period of forcing similar to system time scale, $\omega\tau \sim 1$~~

In the intermediate regime,  $T \sim \tau$ , when the system responds on approximately the same time scale as the period of the forcing the dynamics are a balance between the system's tendency to want to  
185 decay towards the fixed point and the forcing trying to push it away. After some time,  $t \gg \tau$ , the system will settle into an orbit rather than a fixed point due to the similarity of the time scales. Just as there was a bistable region where multiple stable fixed points existed for a single value of  $D_m$  when  $\omega = 0$ , analogously in the case  $T \sim \tau$  multiple stable periodic attractors are possible given a fixed set of values for  $D_m, D_a$  and  $\omega$ . Which one the system settles in depends only on the system's  
190 initial condition  $x(t=0)$ . One also has local bifurcations in this intermediate region, however they are local bifurcations between orbits rather than fixed points. In this intermediate regime, one can neither place the  $D_a \cos(\omega t)$  part of  $D(t)$  in either the slow or fast processes and therefore the assumptions of the usual early warning methods are not strictly valid. However one can still find early warning indicators in such systems and this is what we do in the following section. The system  
195 state  $x$  is plotted against  $D$  and against  $t$  as the blue line in figure 1.

The dynamics of the system described by equation 11 in three different time scale regimes. Forcing parameters are set to  $D_m = 0, D_a = 1/2$ . In the upper panel system state  $x$  is plotted against  $D(t)$ .

The black lines are the nullelines and the coloured lines are the system responses for different periods of forcing. In the lower panel  $x$  is plotted against the number of cycles,  $t/T$ , once the system has reached a steady state. The dotted line is the forcing,  $D(t)$  while the colored lines are the system responses. The red line is for the slow forcing limit,  $\tau \ll T$ ,  $T = 100\pi$  so  $\omega\tau \approx 1/100$ . As the system time scale is much faster than the change in the forcing, the system essentially 'sticks' to the fixed points until they become unstable at the bifurcations and jump to a different attractor. One can regard the system response in two different ways: (i) a single periodic attractor giving a relaxation oscillations in a monostable region. (ii) Tipping between point attractors by crossing local bifurcations in a bistable region. This tipping causes the dynamics to be very nonlinear. The green line is the fast forcing limit,  $T \ll \tau$ ,  $T = \pi/100$  so  $\omega\tau \approx 100$ . There are two possible stable attractors for this set of values. As the system time scale is much slower than the change in the forcing, the system essentially remains static and all the dynamics come from the forcing itself. Although it is hard to see in the figure due to the small amplitude system response, the lag relative to the forcing is  $1/4$  of a cycle and the dynamics are approximately linear. The blue line is the intermediate regime;  $\tau \sim T$ ,  $T = \pi$  so  $\omega\tau \approx 1$  and there are two possible stable attractors for this set of values. As the system time scale is approximately the same as the period of the forcing, the system response is a competition between the system's tendency to decay towards the nulleline and the forcing pushing it away setting up a stable orbit. Notice there is some phase lag and the dynamics look approximately linear.

### 3 Response phase lag and amplification as an early warning of local bifurcations.

We now look at We consider systems that can be described by

$$\dot{x} = f(x) + D(t) \tag{1}$$

where  $f(x)$  is, generally a nonlinear function of the system state scalar variable  $x$ . ~~Our conceptual model, equation 11, was a specific example of such a system. The~~ with forcing  $D(t)$  ~~is given by equation 2. We consider~~ given by

$$D(t) = D_m + D_a \cos(\omega t). \tag{2}$$

$D_m$  and  $D_a$  are constants,  $\omega = \frac{2\pi}{T}$  is the angular frequency and  $T$  is the period of the forcing. We have assumed any other random, noisy external forcing is very small and can be neglected. The solution for a general form for  $D(t)$  is given in the appendix, however here we use simple sinusoidal forcing as this is most relevant for many climate systems and we wish not to obscure the simplicity of the main ~~results~~ result.  $\dot{x}$  describes the dynamics of a forced overdamped system. This is a nonautonomous system whose state can be completely described by  $t$  and  $x$ . After some time  $t_s \gg \tau$  ~~the system~~, where  $\tau$  is the system time scale, the system will settle into some sort of steady

state, either an orbit or a fixed point whose mean state  $\bar{x}$  is

$$\bar{x} = \frac{1}{T} \int_{t_s}^{T+t_s} x(t) dt. \quad (3)$$

We now Taylor expand  $f(x)$  to first order around  $\bar{x}$  so that

$$\dot{x} \approx a - \frac{x}{\tau} + D_a \cos(\omega t). \quad (4)$$

235 where

$$a = f(\bar{x}) - \frac{\partial f}{\partial x} \Big|_{x=\bar{x}} \bar{x} + D_m \quad (5)$$

$$\tau = -1 / \frac{\partial f}{\partial x} \Big|_{x=\bar{x}} \quad (6)$$

are the linearisation constants. We have assumed higher order terms such as  $\frac{1}{n!} \frac{\partial^n f}{\partial x^n} (x - \bar{x})^n$ ,  $n \geq 2$  are small relative to zeroth and first order terms so that the linearised dynamics approximates the

240 full nonlinear dynamics well. We show how to check this approximation in section 2.1. Assuming ~~for the moment that this is a good approximation~~ the approximation is good, one can solve equation ~~4~~ analytically. As  $t \gg \tau$  the system settles into the orbit

$$\lim_{t \gg \tau} x(t) = a\tau + \frac{D_a \tau}{\sqrt{1 + \omega^2 \tau^2}} \cos(\omega t + \phi) \quad (7)$$

where the system response lags the forcing by phase  $\phi_{lag} = \omega t_{lag} = -\phi$  given by

$$245 \phi_{lag} = \arctan(\omega\tau). \quad (8)$$

that is, the phase lag is a function of the forcing frequency and the system response time scale. One also notices that the system response, relative to the forcing amplitude,  $D_a$ , is amplified by a factor

$$\frac{\tau}{\sqrt{1 + \omega^2 \tau^2}} \quad (9)$$

which is also a direct function of  $\omega$  and  $\tau$ . ~~We save the~~ The more general derivation when  $D(t)$  can

250 be any periodic function ~~to appendix A.~~ is given in the appendix A.

## 2.1 ~~Asymptotics of the early warning indicators and examples of systems in these limits~~

### 2.0.1 ~~$\omega\tau \gg 1$ , Terrestrial carbon cycle forced by annual solar insolation~~

~~Consider the asymptotics of equation 8. When the system is losing stability and approaching a local bifurcation its time scale becomes very large,  $\tau \gg T$ , and the system phase lag becomes  $\phi_{lag} \rightarrow \pi/2$ .~~

255 ~~That is, the system response lags the forcing by quarter of a cycle. This limit is also appropriate for systems where the periodic forcing is much quicker than the time scale of the system. Unfortunately, inferring a time scale of a system with  $\phi_{lag} \rightarrow \pi/2$  is not possible to do reliably from the phase lag as  $\phi_{lag}$  asymptotes to this value. One can only reliably conclude  $\tau \gg T$ .~~

260 The system response amplification in the  $\tau \gg T$  limit  $\rightarrow \frac{1}{\omega}$ . That is, system response amplitude is related to the forcing amplitude,  $D_a$ , by  $\frac{D_a}{\omega}$ .

265 An example of a system approximately modelled by this limit is the global terrestrial vegetation carbon which has a dominant timescale on the order of decades, much larger than its periodic forcing, the annual cycle of solar insolation. This dominant time scale comes from the large long term carbon storage e.g. the time scale taken for a forest to regrow once cut down. One sees this phase lag of quarter of a cycle in the annual minimum of the Mauna Loa  $\text{CO}_2$  record<sup>1</sup> relative to the Northern hemisphere solar insolation maximum. This lagged annual minimum in the integrated response of the total atmospheric carbon results from the dominance of the Northern Hemisphere's mid-latitude terrestrial vegetation carbon in the global carbon flux. We have plotted the Mauna Loa  $\text{CO}_2$  record and the time of year of the minimum concentration in figure 8.

270 Atmospheric  $\text{CO}_2$  concentration recorded at Mauna Loa against time in the upper panel. In the lower panel we have plotted the minimum annual  $\text{CO}_2$  concentration against year. One notices the minimum  $\text{CO}_2$  concentration occurs roughly 3/4 of the way through the year. This is because maximal carbon uptake occurs during the Northern hemisphere summer from the terrestrial vegetation and it is maximally lagged behind the maximum in the Northern hemisphere solar insolation (best growing conditions) by 1/4 of a cycle because of the time scale difference between the response of the system and the period of the forcing. In this case the system is the terrestrial vegetation which has a timescale of decades and the periodic forcing is the annual cycle of solar insolation.

### 2.0.1 $\omega\tau \ll 1$ , Ice sheet dynamics forced by Milankovitch cycles

When  $T \gg \tau$ , there is no phase lag,  $\phi_{lag} \rightarrow 0$ , and the system can respond instantly.

280 The system response amplitude in this limit  $\rightarrow \tau$ . That is, system response amplitude is related to the forcing amplitude,  $D_a$ , by  $D_a\tau$ .

285 An example of a system that has the correct time scale separation and periodic forcing are the glacial/interglacial cycles that have the slow build, fast collapse type behaviour of relaxation oscillations. Ice sheets have time scales in the order of thousands of years forced by the solar insolation variation of Milankovitch cycles. The forcing is a superposition of many different sinusoidal frequencies, the dominant ones having periods of 41 kyr (related to the obliquity of Earth's orbit), 19 and 23 kyr (related to the precession). Current thinking however, favours more complex, two and higher dimensional dynamics to model these cycles than the single variable models we consider in this paper (Saltzman (2002), Crucifix (2012), Saedeleer et al. (2013), and Crucifix (2013)).

### 290 2.0.1 $\omega\tau \sim 1$ , Ocean mixed layer temperature forced by annual solar insolation

---

<sup>1</sup>Dr. Pieter Tans, NOAA/ESRL ([www.esrl.noaa.gov/gmd/ccgg/trends/](http://www.esrl.noaa.gov/gmd/ccgg/trends/)) and Dr. Ralph Keeling, Scripps Institution of Oceanography ([scrippsco2.ucsd.edu/](http://scrippsco2.ucsd.edu/))

The intermediate regime, when  $\tau \sim T$  (the time scale of the system is approximately the same as the forcing period) is where phase lag and response amplification are most useful as early warning indicators as one sees values somewhere between the two limits.

295 To give an example of a system operating in this regime consider the annual variation in sea temperatures in northern hemisphere temperate regions. A rough estimate of the ocean surface mixed layer time scale gives  $\tau \sim 10$  months and this surface layer is heated by the annual cycle of solar insolation to varying degrees throughout the year. Calculation of the phase lag for this  $\tau$  and  $T$  yields a lag of about 2.6 months i.e. roughly the maximal and minimal sea temperatures are in September and March. Arctic sea ice extent also falls into this regime and will be one of the systems we apply  
300 the early warning indicators to in section ??.

### 3 System nonlinearity from Fourier analysis

#### 2.1 System nonlinearity and harmonic amplitude from Fourier analysis

By simply looking at the time series of the system response and the forcing one can determine what the amplitude and phase lag are when the driving is of the form equation 2 and the system  
305 response is approximately linear without the need for statistics. However, the system is essentially nonlinear and these nonlinear effects may become large near a bifurcation or when the system is driven hard. By taking the Fourier transform of the time series of the system response one can quantify how large these nonlinear effects are. With a similar motivation Wiesenfeld (1985) and Wiesenfeld and McNamara (1986) calculated the Fourier spectra of the perturbations, rather than the response, away from periodic attractors very close to local bifurcations with noisy and weak  
310 periodic modulation respectively.

Once the system has settled into an orbit of period  $T$ , ~~we can write~~ the full nonlinear response of an arbitrary system can be written as a Fourier series, a sum of  $N$  sinusoidal functions with angular frequencies  $\omega_n = \frac{2\pi n}{T}$ , amplitudes  $A_n$  and phases  $\phi_n$  i.e.

$$315 \quad x(t) = \sum_{n=0}^N A_n \cos(\omega_n t + \phi_n). \quad (10)$$

The  $n = 0$  component is a constant, the long term mean of the response, the  $n = 1$  component is the linear response of the system and the  $n \geq 2$  components are the  $n$ th order harmonics and come about from the nonlinear response of the system. Since the system has settled into a periodic orbit the system must repeat itself every cycle. The only way the system can do this is by adding harmonics  
320 to linear response. By looking at the ratios  $\frac{A_n}{A_1}$  for  $n \geq 2$  ~~we can see how important~~ the nonlinear effects ~~are~~ relative to the linear approximation can be quantified. In practice the largest harmonics will generally be the 2nd ( $n = 2$ ) and 3rd order ( $n = 3$ ) harmonics and provided they are an order of magnitude (10 times,  $\frac{A_n}{A_1} < 10^{-1}$ ) less than the fundamental harmonic, the linear analysis in the last

section works well. Calculation of the amplitudes,  $A_n$ , can be made via a Fourier transform of the time series.

325

One may also expect subharmonics, components that have periods that are integer multiples of the forcing period, to be observed in the system response. Subharmonics are not possible in the systems we consider here due to the dimensionality of the phase space.<sup>1</sup>

~~Calculation of the amplitudes,  $A_n$ , is via a Fourier transform of~~ Since the ratios  $\frac{A_n}{A_1}$  measure how nonlinear the system is one expects these to increase as the system approaches a bifurcation. These ratios can be plotted for a time series by taking the Fourier transform for a data window consisting of an integer number of cycles and sliding this window forward by one cycle recursively through the time series. To do this, we choose to represent the system response, equation 10, in the more convenient but equivalent form-

330

$$x(t) = \sum_{n=-N}^N c_n e^{i\omega_n t}$$

335

~~where we have defined  $c_n = \frac{A_n}{2} e^{i\phi_n}$  and  $c_{-n} = c_n^*$ . We then take the Fourier transform of this form to find the  $c_n$~~

$$c_n = \frac{1}{T} \int_0^T x(t) e^{-i\omega_n t} dt$$

~~so the amplitude  $A_n$  associated to the  $n$ th harmonic is given by-~~

$$A_n = 2|c_n|.$$

340

~~One can also find the phases,  $\phi_n$  by taking the argument of  $c_n$ .~~ The number of cycles in the window must be large enough that the harmonics can be satisfactorily resolved in the Fourier spectra. In addition, each cycle must be sampled at a time interval  $\Delta t < T_{Nyquist}/2$  where  $T_{Nyquist}$  is the minimum harmonic period you want to resolve.

345

~~Since the ratios  $\frac{A_n}{A_1} = \frac{|c_n|}{|c_1|}$  measure how nonlinear the system is one expects these to increase as the system approaches a bifurcation as well as quantitative measures of how appropriate the linear analysis is. We demonstrate the linear early warning indicators and the Fourier analysis in the next section.~~

---

<sup>1</sup>Systems described by equation 1 are completely described by the two dimensional space of variables  $x$  and  $t$ . Recasting the nonautonomous system in equation 1 as a two dimensional autonomous system by identifying a new angular variable  $\phi = \omega t$ , the system is then described by  $\dot{x} = f(x) + D(\phi)$  and  $\dot{\phi} = \omega$ . The resulting phase space  $(x, \phi)$  is then cylindrical as  $\phi$  is  $2\pi$  modular. If subharmonics are possible in the periodic system response the trajectory must wind around the cylinder at least twice before repeating itself. Such a trajectory implies it crosses itself which is not allowed due to the existence and uniqueness theorem. Therefore subharmonics cannot exist in the two dimensional systems. This is of course not true for three and higher dimensional systems.



## 2.2 Lag 1 autocorrelation of a return map

350 Provided the system time scale is larger than its period,  $\tau/T > 1$ , one can use return maps to assess the stability of a periodic attractor. The return map time series, generated by sampling the system response once every cycle, allows one to apply fixed point statistical early warning indicators such as lag 1 autocorrelation. It is noisy, random forcing away from the periodic attractor that this method infers time scale from, rather than response to deterministic, periodic forcing. This is usually done  
355 by calculating the lag 1 autocorrelation for a sliding data window of the return map time series at least as long as the system time scale but not so long that any increasing trend in system time scale skews the autocorrelation estimate. It is also desirable to have many points within this window as the standard error of the estimate scales as  $1/\sqrt{m}$  where  $m$  is the number of cycles (points) within the window (see Williamson and Lenton (2015) for a discussion). For time series consisting of a small  
360 number of cycles this can be a limiting factor.

## 3 Examples

We now demonstrate the early warning indicators in section 2 for different ratios of forcing period,  $T$ , (or equivalently angular frequency  $\omega$ ) to system time scale  $\tau$ . In particular, we use a periodically forced double well potential as our main system. This system has been extensively studied in the  
365 context of stochastic resonance (see McNamara and Wiesenfeld (1989) and Gammaitoni et al. (1998) for reviews) as the simplest model of the phenomena when noise is also added. Phase and amplitude have been investigated in this setting by Shneidman et al. (1994) and Jung and Hänggi (1993). This literature is largely concerned with resonance effects in transition probabilities between the wells (finite barrier height between the wells) rather than the anticipation of local bifurcations (barrier  
370 height tends to zero) that is the central interest here.

### 3.1 ~~Conceptual model~~

~~We now demonstrate how one might use these indicators to detect changing~~ Our system which has one dynamical variable,  $x$ , and evolves according to

$$\dot{x} = x - x^3 + D(t) \tag{11}$$

375 where overdots denote differentiation with respect to time,  $t$  and the periodic forcing function  $D(t)$  is given by equation 2. Equation 11 models a nonautonomous nonlinear system, the overdamped limit of a Duffing oscillator (Thompson and Stewart (2002)). When forcing is constant ( $\omega = 0$ ) the familiar, well studied autonomous fold bifurcation is recovered (for example see Strogatz (2001)). For  $\omega = 0$ , the solutions of  $\dot{x} = 0$ , give the system's fixed points,  $x^*$  (the nullclines) and number  
380 either one or three depending on the value of  $D_m$ . One can evaluate the stability of these fixed points

by looking at the linearized dynamics close to the fixed points,  $J(x^*)$

$$J(x^*) = \left. \frac{\partial \dot{x}}{\partial x} \right|_{x=x^*} = 1 - 3x^{*2} \quad (12)$$

If  $J(x^*)$  is negative, the fixed point is stable, if it is positive it is unstable. In the region where three fixed points exist one finds a bistable region i.e. two points are stable while the third is unstable. The 385 bistable region has boundaries marked by the local bifurcations and these can be found by solving  $J(x^*) = 0$  for  $x^*$  when the fixed point becomes neutrally stable. One can also calculate the  $\epsilon$ -folding time scale of the system in state  $x$ ,  $\tau$  from the Jacobian  $\tau = -1/J(x)$ . We will refer to the  $\epsilon$ -folding time as the system time scale (equivalently changing system stability) and therefore the anticipation of an approaching local bifurcation. We demonstrate this with the conceptual system in equation 390 11. ~~We assume the~~. As the system gets closer to the bifurcation the system time scale will increase and tend to infinity at the bifurcation. Early warning indicators are simply functions of  $J(x^*)$  or equivalently  $\tau$ .

### 3.1 Period of forcing similar to system time scale, $\omega\tau \sim 1$

This regime,  $T \sim \tau$ , is the main focus study in this manuscript, when the system responds on 395 approximately the same time scale as the period of the forcing. In this regime the dynamics are a balance between the system's tendency to want to decay towards the fixed point and the forcing trying to push it away. After some time,  $t \gg \tau$ , the system will settle into an orbit rather than a fixed point due to the similarity of the time scales. Just as there was a bistable region where multiple stable fixed points existed for a single value of  $D_m$  when  $\omega = 0$ , analogously in the case  $T \sim \tau$  400 multiple stable periodic attractors are possible given a fixed set of values for  $D_m$ ,  $D_a$  and  $\omega$ . The system state  $x$  is plotted against  $D$  and against  $t$  as the blue line in figure 1. Which state the system settles in depends only on the system's initial condition  $x(t = 0)$ . Local bifurcations are present in this intermediate region, however they are local bifurcations between orbits rather than fixed points. In this intermediate regime, one can neither place the  $D_a \cos(\omega t)$  part of  $D(t)$  in either the slow or 405 fast processes and therefore the assumptions of the usual fixed point early warning methods are not strictly valid. This is however where phase lag and response amplification are useful early warning indicators.

To illustrate the early warning indicators we fix the forcing amplitude  $D_a$  and the period  $T \sim O(\tau)$  ~~are fixed and~~ and take  $D_m$  ~~is as~~ as a control parameter, slowly varying from negative values towards 410 the local bifurcation in the system described by equation 11. We expect to see the system response become more phase lagged and amplified as we approach the local bifurcation at  $D_m \approx 0.33$  when approaching from the lower nullcline solutions. We also expect the amplitude of the harmonics of the system response to increase.

~~In our example we~~ We choose to tip the system from one state to another by slowly altering the 415 mean of the driving  $D_m$ . ~~We could, however, have tipped the system~~ Alternatively, the system could

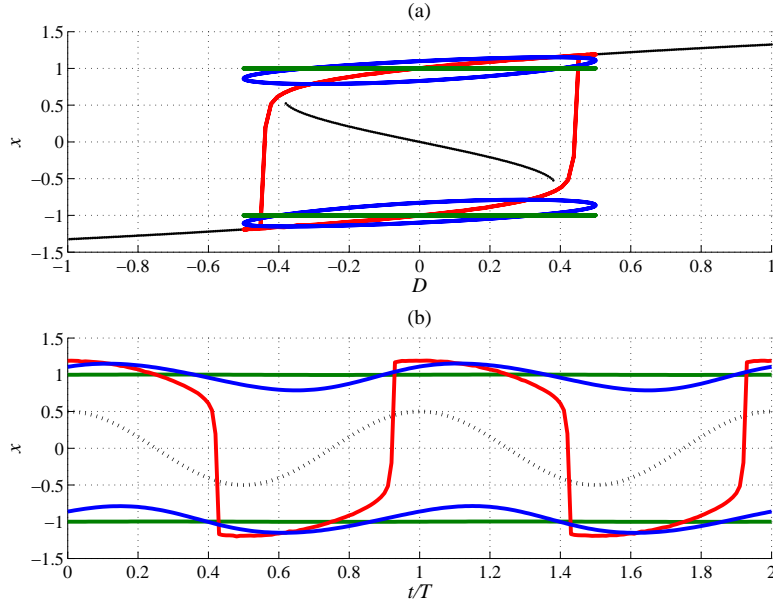


**Figure 1.** The dynamics of the system described by equation 11 in three different time scale regimes. Forcing parameters are set to  $D_m = 0$ ,  $D_a = 1/2$ . In the upper panel system state  $x$  is plotted against  $D(t)$ . The black lines are the nullclines and the coloured lines are the system responses for different periods of forcing. In the lower panel  $x$  is plotted against the number of cycles,  $t/T$ , once the system has reached a steady state. The dotted line is the forcing,  $D(t)$  while the colored lines are the system responses. The red line is for the slow forcing limit,  $\tau \ll T$ ,  $T = 100\pi$  so  $\omega\tau \approx 1/100$ . As the system time scale is much faster than the change in the forcing, the system essentially ‘sticks’ to the fixed points until they become unstable at the bifurcations and jump to a different attractor. One can regard the system response in two different ways: (i) a single periodic attractor giving a relaxation oscillations in a monostable region. (ii) Tipping between point attractors by crossing local bifurcations in a bistable region. This tipping causes the dynamics to be very nonlinear. The green line is the fast forcing limit,  $T \ll \tau$ ,  $T = \pi/100$  so  $\omega\tau \approx 100$ . There are two possible stable attractors for this set of values. As the system time scale is much slower than the change in the forcing, the system essentially remains static and all the dynamics come from the forcing itself. Although it is hard to see in the figure due to the small amplitude system response, the lag relative to the forcing is  $1/4$  of a cycle and the dynamics are approximately linear. The blue line is the intermediate regime,  $\tau \sim T$ ,  $T = \pi$  so  $\omega\tau \approx 1$  and there are two possible stable attractors for this set of values. As the system time scale is approximately the same as the period of the forcing, the system response is a competition between the system’s tendency to decay towards the nullcline and the forcing pushing it away setting up a stable orbit. Notice there is some phase lag and the dynamics look approximately linear.

have tipped by changing one of the other driving parameters such as amplitude  $D_a$  or frequency  $\omega$ . Since the system response amplitude depends on  $D_a$  and  $\omega$  and phase lag depends on  $\omega$ , one must take this into account when inferring system time scales from the indicators.

In figure 2 ~~we run the system~~ the system is run forward in time, linearly varying  $D_m$  from -2  
420 to 2 across the bifurcation over about 25 cycles of the forcing period (for the values of the pa-  
rameters see the figure caption). ~~In figure 3 we have plotted the~~ Plotted in figure 3 are phase lag  
and amplitude of the system response prior to the bifurcation at around  $t/T = 15$  ~~which are both,~~  
Both are increasing as the bifurcation is approached due to the increase in  $\tau$ . Phase lag is calcu-  
425 lated from the difference between the times of the maxima in the forcing and the system response in  
each cycle. Response amplitude is calculated by taking half the difference between the maximal and  
minimal values in the system response in each cycle. Also plotted are the ratios of the second and  
third harmonic amplitudes to the amplitude of the fundamental harmonic with time using a sliding  
window of length 5 complete cycles against the time at the end of the sliding window. The window  
needs to be long enough to resolve the harmonics in the spectrum but short enough to keep  $D_m$   
430 approximately constant. For this example, where the harmonic amplitudes (and the nonlinearity of  
the response) are quite small, 5 cycles is the minimum to resolve the peaks. The sliding window is  
then advanced one cycle in the time series and the harmonic amplitudes are calculated for this new  
window. This process is iterated until the local bifurcation is reached to produce the lower panel in  
figure 3 which shows both harmonic amplitudes increasing.

435 We also plot the complete spectrum of the ratios  $A_n/A_1$  against  $T_n/T$  derived from a Fourier  
transform of the system response in figure 4. In the upper panel all parameters are the same as figure  
2 except we have fixed  $D_m$  in each of the two runs. In the first run  $D_m = -2$ , this is far from  
the bifurcation and one expects the system to behave more linearly (blue line). One sees a second  
harmonic around 2 orders of magnitude smaller than the linear response. In the second run  $D_m =$   
440 0.25 and the orbit is much closer to the bifurcation (red line). The second harmonic has increased  
to about an order of magnitude smaller than the fundamental harmonic and a third harmonic is now  
also visible indicating the system has become more nonlinear.

~~We illustrate the spectrum of very nonlinear dynamics in the lower panel of figure 4. This is the~~  
~~spectrum of the slow forcing run with the same parameters in figure 1 (red line) that had a response~~  
445 ~~that resembled~~

To give an example of a climate system operating in this regime consider the annual variation in  
sea temperatures in northern hemisphere temperate regions. A rough estimate of the ocean surface  
mixed layer time scale gives  $\tau \sim 10$  months and this surface layer is heated by the annual cycle of  
solar insolation to varying degrees throughout the year. Calculation of the phase lag for this  $\tau$  and  
450  $T$  yields a lag of about 2.6 months i.e. roughly the maximal and minimal sea temperatures are in  
September and March. Arctic sea ice extent also falls into this regime and we analyze this system in  
section 4.

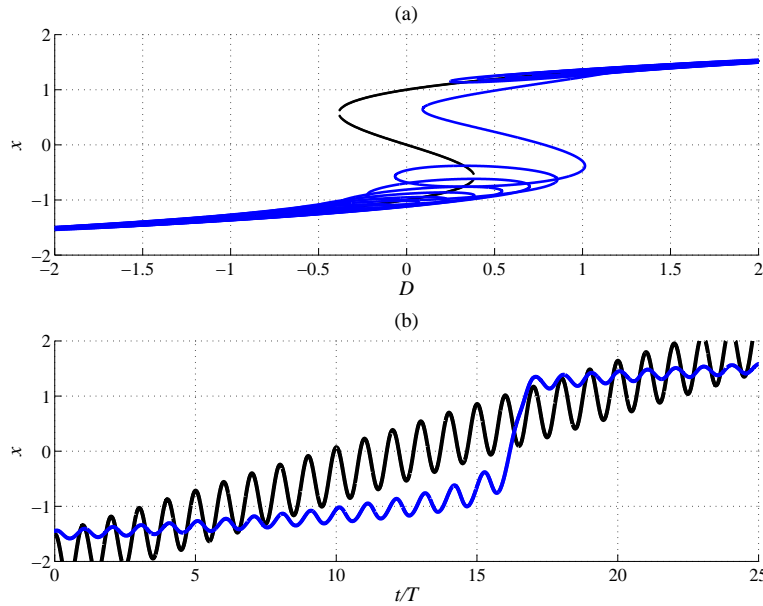


**Figure 2.** The dynamics of the system are described by equation 11 with varying  $D_m$ . Parameters are set to  $D_a = 1/2$ ,  $T = \pi$  (the same order as the system time scale  $\omega T \sim 1$ ) and  $D_m$  is varied linearly with time between -2 and 2 over about 25 cycles. In the upper panel the black lines are the nullclines while the system response is the blue line plotted against  $D(t)$ . The orbit loses stability around a mean value of  $D \approx 0.5$  and jumps to a new orbit. In the lower panel we have plotted the system response (blue) against the forcing  $D$  against  $t/T$ . One can see the loss of stability of the orbit around  $t/T \approx 15$  and the prior increase in system response amplitude.

### 3.1.1 A note about return maps

455 Towards the upper range of  $\omega T \sim 1$ , specifically  $\omega T > 2\pi$ , return map analysis via statistical fixed  
point indicators becomes useful with the added caveat that the time series of the system must have  
enough cycles to produce statistically significant results. Return map analysis is complementary to  
phase lag and response amplification since these quantities start to asymptote when  $\omega T > 2\pi$ . This  
complementarity is illustrated in the following figures. The blue line in figure 5 is essentially the  
same as figure 2 ( $\omega T \sim 1$ ) except  $D_m$  is varied over 100 cycles instead of 25. This is because extra  
460 data points are needed to calculate the lag 1 autocorrelation of the return maps with any reliability.  
We have also added Gaussian white noise to equation 11 of standard deviation 0.01 as the return  
map method needs small perturbations with which to infer return times to the cycle. In figure 6 we  
have plotted the early warning indicators for this time series including the return map calculated with  
a sliding window of 25 cycles. The black lines are the theoretical curves and the blue lines are the  
465 estimated curves. The key point is the theory and estimated autocorrelations do not show anything  
in this regime ( $\omega T \sim 1$ ) however the phase lag and response amplification are clearly increasing.

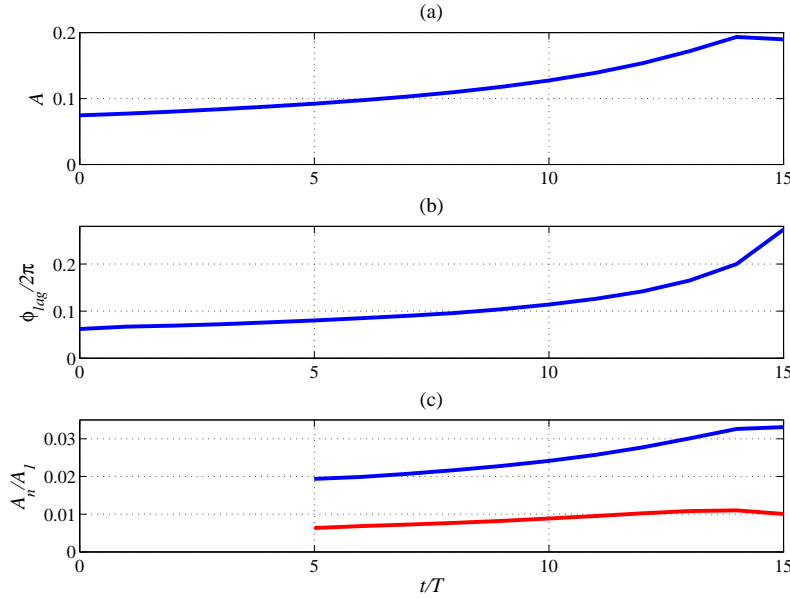


**Figure 3.** The early warning indicators, response amplification (upper panel),  $A = \frac{D_a \tau}{\sqrt{1 + \omega^2 \tau^2}}$ , and phase lag (lower-middle panel),  $\frac{\phi_{lag}}{2\pi} = \frac{1}{2\pi} \arctan(\omega\tau)$  calculated for the time series in figure 2. We have plotted these indicators prior to the bifurcation at  $t/T \approx 15$ . ~~Note both~~ The 2nd (blue) and 3rd (red) harmonic amplitudes  $A_n/A_1$  are also plotted in the lower panel using a sliding window of 5 complete cycles. All indicators are increasing as ~~one would expect~~ expected.

Conversely, the red lines in figure 5 and 7 are the same quantities but with decreased period of forcing ( $T = 1/4$  so  $\omega\tau \sim 4\pi$ ). This is a regime in which phase lag and response amplitude start to asymptote and are therefore not so useful to infer changing system time scale. However, lag 1 autocorrelation of the return map now becomes useful as can be seen in figure 7.

### 3.2 Period of forcing much slower than system time scale, $\omega\tau \ll 1$

When equation 11 is operating in this regime (period of forcing much greater than system time scale  $T \gg \tau$ ) the system can adjust to changing  $D(t)$  relatively quickly and effectively remains at a fixed point.  $D(t)$  can therefore be modelled as a slow constant, control parameter and all the usual time scale separation assumptions apply. Fixed point indicators such as lag 1 autocorrelation are then good early warning indicators of local bifurcations. In contrast, phase lag and response amplitude are not useful as these quantities asymptote to  $\phi_{lag} \rightarrow 0$  and  $\rightarrow \tau$  respectively. The system state  $x$  is plotted against  $D$  and against  $t$  as the red line in figure 1.

An example of a system that has the correct time scale separation and periodic forcing are the glacial/interglacial cycles that have the slow build, fast collapse type behaviour of relaxation oscillations. For these parameters the dynamics is very nonlinear as shown by the large amplitude of the

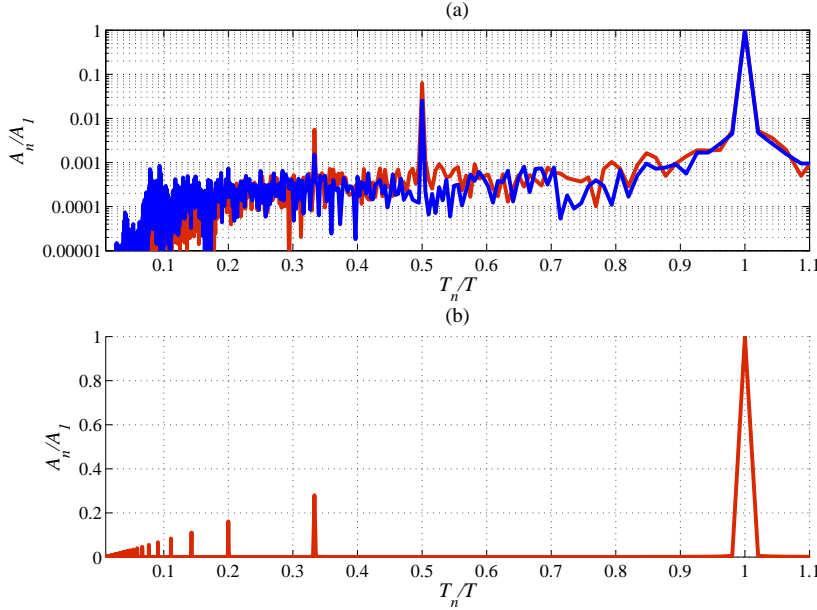


**Figure 4.** Ratio of the  $n$ th order harmonic amplitude to the fundamental harmonic amplitude  $A_n/A_1$  against the ratio of the  $n$ th harmonic period to the fundamental harmonic period  $T_n/T$ . The dynamics of the system are described by equation 11. In the upper panel parameters are fixed to  $D_a = 1/2$ ,  $T = \pi$  (the same order as the system time scale  $\tau$ ). The blue line is for  $D_m = -2$  (far away from the bifurcation), the nonlinear response is dominated by the second harmonic at  $T_n/T = 1/2$  although small, about two orders of magnitude less than the linear response. The red line is  $D_m = 1/4$ , close to the bifurcation the system response has become more nonlinear. The second harmonic ( $T_n/T = 1/2$ ) is now almost one order of magnitude less and the third order harmonic ( $T_n/T = 1/3$ ) is also prominent. In the bottom panel, we show the spectrum when the dynamics is very nonlinear. Parameters are set to  $D_m = 0$ ,  $D_a = 1/2$ ,  $T = 100\pi$  so  $\omega\tau \approx 1/100$ . This is the slow forcing limit shown in figure 1 (red line) which has a very nonlinear relaxation oscillation type response. Note only odd harmonics ( $T_n/T = 1/3, 1/5, 1/7, \dots$  etc.) are present due to the system experiencing a symmetric potential requiring the solution,  $x(t)$ , to also have this symmetry.

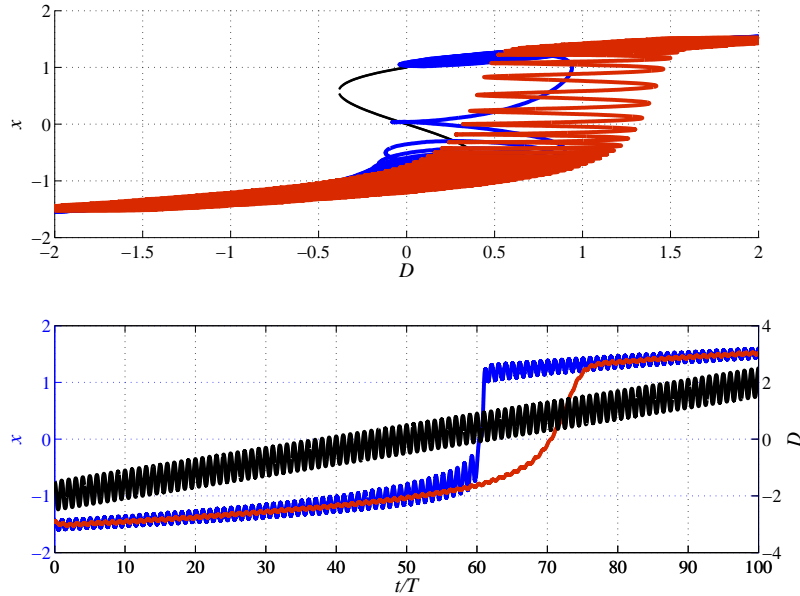


**Figure 5.** Same figure as figure 2 in the manuscript except the variation of  $D_m$  is over more cycles to generate more points for a reliable return map analysis. Weak Gaussian white noise of standard deviation 0.01 is added to the system. Parameters are set to  $D_a = 1/2$  and  $D_m$  is varied linearly with time between -2 and 2 over about 100 cycles. In the upper panel the black lines are the nullclines while the system response is the blue line for  $T = \pi$  giving  $\omega\tau \sim 1$  whereas the red line has a shorter period of  $T = 1/4$  to give  $\omega\tau \sim 4\pi$ . These are plotted against  $D(t)$ . In the lower panel we have plotted these system responses as time series against the forcing (black line).

485 ~~harmonics. Notice only~~ Ice sheets have time scales in the order of thousands of years forced by the solar insolation variation of Milankovitch cycles. The forcing is a superposition of many different sinusoidal frequencies, the dominant ones having periods of 41 kyr (related to the obliquity of Earth's orbit), 19 and 23 kyr (related to the precession). Current thinking however, favours more complex, two and higher dimensional dynamics to model these cycles than the single variable models we consider in this paper (Saltzman (2002), Crucifix (2012), Saedeleer et al. (2013), and Crucifix (2013)).

490 The spectrum of a very nonlinear, relaxation oscillation type, dynamics is illustrated in the lower panel of figure 4. This is the spectrum of the slow forcing run (red line) in figure 1. Only odd harmonics appear in its spectrum ~~-This is~~ because the static potential  $V = -\int \dot{x} dx$  is symmetric about  $x$  for this value of  $D_m = 0$  i.e.  $V(x) = V(-x)$  and therefore any solution of  $\dot{x}$  must also have this symmetry,  $x(t + T/2) = -x(t)$ . Only odd harmonics have this property.<sup>2</sup>

<sup>2</sup>This is not sufficient though as there are other parameter settings that feature the second harmonic and also have the same symmetric potential i.e.  $D_m = 0$  and  $T = \pi$  in figure 1 (blue line). The difference is that the runs featuring second harmonic



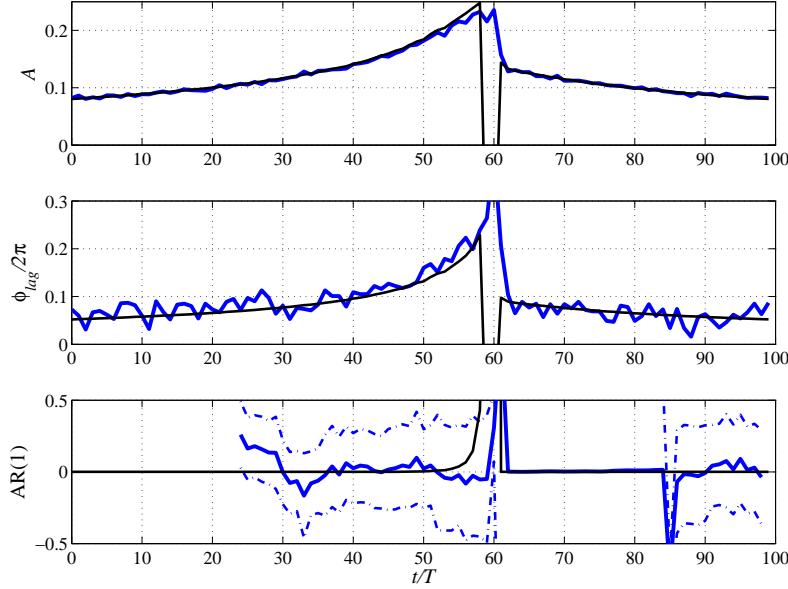


**Figure 6.**  $\omega\tau \sim 1$ : The early warning indicators, response amplification (upper panel),  $A = \frac{D_a\tau}{\sqrt{1+\omega^2\tau^2}}$ , and phase lag (middle panel),  $\frac{\phi_{lag}}{2\pi} = \frac{1}{2\pi} \arctan(\omega\tau)$  calculated for the blue time series in figure 5. In the lower panel, lag 1 autocorrelation of a sliding window of 25 points of the return map is plotted with standard errors (dashed lines) on the estimate. Black lines are theoretical curves of all the quantities. The key point is phase lag and amplitude response are useful quantities in this regime however the return map is not.

### 3.3 Period of forcing much faster than system time scale, $\omega\tau \gg 1$

495 The system state  $x$  is plotted against  $D$  and against  $t$  as the green line in figure 1. The forcing is  
 changing much faster than the system can respond so the system effectively looks static and all  
 the dynamics come from the forcing directly. In this case we can place  $D(t)$  in the fast dynamics.  
 However, not all of the other assumptions for use of lag 1 autocorrelation in a fixed point analysis  
 are satisfied. It is true that  $D(t)$  is independent of  $x$ , however it is not uncorrelated with itself at  
 500 different times and therefore cannot strictly be modelled as a normally distributed random variable,  
 although at first glance it looks as though it is again possible to use usual fixed point early warning  
 techniques so one must be careful. In this regime, phase lag and response amplification asymptote  
 and again are not very useful to detect a trend in increasing time scale. Phase lag,  $\phi_{lag} \rightarrow \pi/2$  and  
 response amplification  $\rightarrow \frac{1}{\omega}$  so one may only infer  $\tau \gg T$ .

responses only experience a limited part of the potential, not the full symmetric potential. Even though the potential is the same, the forcing is quick enough to trap the system in an orbit in just one of the two potential wells. This local potential well is asymmetric and what the system sees is effectively described by a Taylor expansion around the centre of that well. In contrast the relaxation oscillation type run travels across both wells equally and therefore sees the global symmetric potential requiring an odd harmonic solution. This is not a generic case however.

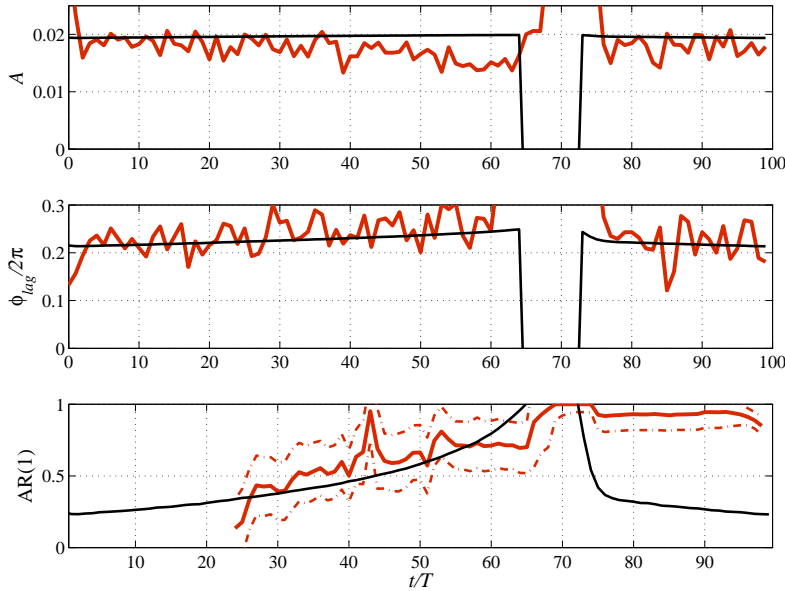


**Figure 7.**  $\omega T \sim 4\pi$ : The early warning indicators, response amplification (upper panel),  $A = \frac{D_a \tau}{\sqrt{1 + \omega^2 \tau^2}}$ , and phase lag (middle panel),  $\frac{\phi_{lag}}{2\pi} = \frac{1}{2\pi} \arctan(\omega T)$  calculated for the red time series in figure 5. In the lower panel, lag 1 autocorrelation of a sliding window of 25 points of the return map is plotted with standard errors (dashed lines) on the estimate. Black lines are theoretical curves of all the quantities. Phase lag and amplitude response have now asymptoted and are not useful quantities however the return map now becomes useful.

505 An example of a system approximately modelled by this limit is the global terrestrial vegetation carbon which has a dominant timescale on the order of decades, much larger than its periodic forcing, the annual cycle of solar insolation. This dominant time scale comes from the large long term carbon storage e.g. the time scale taken for a forest to regrow once cut down. One sees this phase lag of quarter of a cycle in the annual minimum of the Mauna Loa CO<sub>2</sub> record<sup>3</sup> relative to the Northern  
 510 hemisphere solar insolation maximum. This lagged annual minimum in the integrated response of the total atmospheric carbon results from the dominance of the Northern Hemisphere's mid latitude terrestrial vegetation carbon in the global carbon flux. We have plotted the Mauna Loa CO<sub>2</sub> record and the time of year of the minimum concentration in figure 8.

<sup>3</sup>Dr. Pieter Tans, NOAA/ESRL ([www.esrl.noaa.gov/gmd/ccgg/trends/](http://www.esrl.noaa.gov/gmd/ccgg/trends/)) and Dr. Ralph Keeling, Scripps Institution of Oceanography ([scrippsco2.ucsd.edu/](http://scrippsco2.ucsd.edu/))

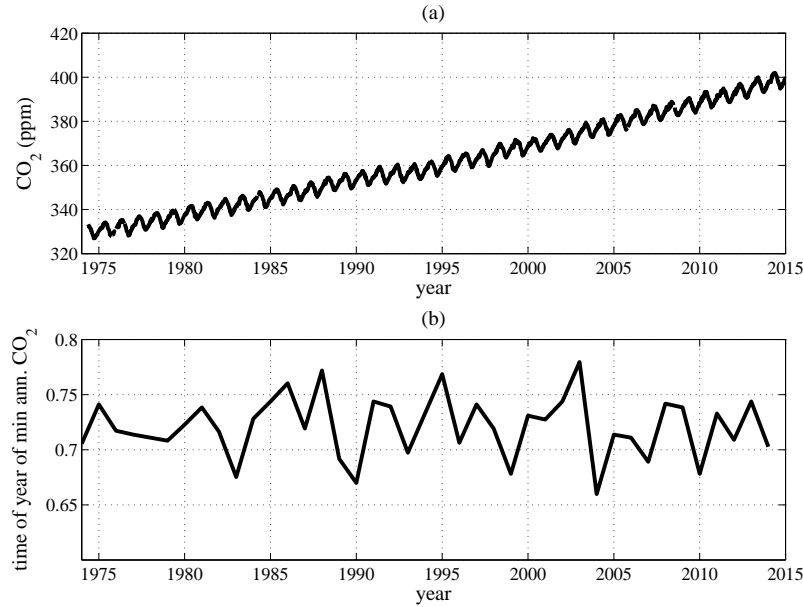


**Figure 8.** ~~Ratio of the  $n$ th order harmonic amplitude to the fundamental harmonic amplitude  $A_n/A_1$~~  Atmospheric CO<sub>2</sub> concentration recorded at Mauna Loa against ~~the ratio of the  $n$ th harmonic period to the fundamental harmonic period  $T_n/T$ .~~ The dynamics of the system are described by equation 11. Parameters are fixed to  $D_a = 1/2$ ,  $T = \pi$  (the same order as the system time scale  $\tau$ ) for in the upper panel. The blue line is for  $D_m = 2$  (far away from in the bifurcation), lower panel we have plotted the nonlinear response is dominated by minimum annual CO<sub>2</sub> concentration against year. One notices the second harmonic at  $T_n/T = 1/2$  although small, about two orders minimum CO<sub>2</sub> concentration occurs roughly 3/4 of magnitude less than the linear response way through the year. The red line This is  $D_m = 1/4$ , close to because maximal carbon uptake occurs during the bifurcation Northern hemisphere summer from the system response has become more nonlinear. The second harmonic ( $T_n/T = 1/2$ ) is now almost one order of magnitude less terrestrial vegetation and the third order harmonic ( $T_n/T = 1/3$ ) it is also prominent. In maximally lagged behind the bottom panel, we show the spectrum when the dynamics is very nonlinear. Parameters are set to  $D_m = 0$ ,  $D_a = 1/2$ ,  $T = 100\pi$  so  $\omega\tau \approx 1/100$ . This is the slow forcing limit shown maximum in figure 1 the Northern hemisphere solar insolation (red line best growing conditions) which has by 1/4 of a very nonlinear relaxation oscillation type cycle because of the time scale difference between the response. Note only odd harmonics ( $T_n/T = 1/3, 1/5, 1/7, \dots$  etc.) are present due to of the system experiencing a symmetric potential requiring and the solution,  $x(t)$ , to also have this symmetry period of the forcing.

### 3.4 Arctic sea ice satellite observations

#### 515 4 Looking for a tipping point in Arctic sea ice satellite observations

There has been much research ~~in to on~~ a possible local bifurcation and tipping point in the Arctic sea ice ~~without a clear consensus emerging~~, see for example Armour et al. (2011), Eisenman and Wettlaufer (2009), Lindsay and Zhang (2005), Livina and Lenton (2013), Ridley et al. (2012) and Wang and Overland (2012). This possible bifurcation in the sea ice cover may be due to the well known ice albedo feed-  
520 back first studied by Budyko (1969) and Sellers (1969). When ice is present it reflects a high proportion of the incoming solar radiation due to its higher albedo yet when it starts receding the darker ocean absorbs more radiation increasing heating and promoting more sea ice retreat. This feedback can result in instability and multiple steady states.

We ~~analyze~~ calculate all the previously mentioned early warning indicators for a time series of  
525 Arctic sea ice area satellite observations from 1979 to present ~~data and calculate the day. That is we~~ calculate phase lag, response amplitude ~~and spectrum of the time series~~, relative size of the 2nd and 3rd harmonics and the lag 1 autocorrelation of the return map with time to look for signs of critical slowing down ~~that might indicate the approach of a local bifurcation or 'tipping point' in the Arctic sea-ice. We also calculate the complete Fourier spectra for the entire time series as a linearity check.~~  
530 In figure 9 ~~we have plotted the satellite observations of~~ Arctic sea ice area are plotted against year. Sea ice area data were obtained from The Cryosphere Today project of the University of Illinois. This ~~dataset~~ data set<sup>4</sup> uses SSM/I and SMMR series satellite products and spans 1979 to present at daily resolution.

In figure 10 we plot the amplitude of the sea ice area annual cycle and the phase lag between  
535 the sea ice area minimum and maximum during each cycle. We assume the maximal and minimal driving occurs at the same time as maximal and minimal of the solar insolation, that is, the midpoint and end point of the year respectively to obtain phase lags. To limit the the impact of high frequency variability on the location of the extrema, we have smoothed the daily data with a sliding window ~~with of~~ 30 days.

540 From figure 10 we see the cycle amplitude is increasing with time although the phase lag does not appreciably change. We first make some rough calculations to see if these plots are consistent with each other: From the phase lag figure, a time scale of  $\tau \sim [0.33, 0.5]$  yr from the lag of  $[0.18, 0.2]$  of a cycle can be inferred. If we assume for the moment ~~;~~ the amplitude of the forcing  $D_a$  is not changing throughout the time period of the observations (this may not be true) and take the smallest  
545 value in the range for  $\tau_{1978} = 0.33$  yr ~~at~~ occurring in 1978 and the largest value in 2015,  $\tau_{2015} = 0.5$  yr we can make a rough calculation of how much the sea ice amplitude would have increased i.e.  
$$\frac{A_{2015}}{A_{1978}} = \frac{\tau_{2015}}{\tau_{1978}} \sqrt{\frac{1+\omega^2\tau_{1978}^2}{1+\omega^2\tau_{2015}^2}} \approx 1.06.$$
 From figure 10 we take the amplitude at 1978 to be  $A_{1978} \sim 4.5$  and at 2015 to be  $A_{2015} \sim 5$  we find  $\frac{A_{2015}}{A_{1978}} = 1.11$ . These values could therefore be consistent with a

<sup>4</sup><http://arctic.atmos.uiuc.edu/cryosphere/timeseries.anom.1979-2008>

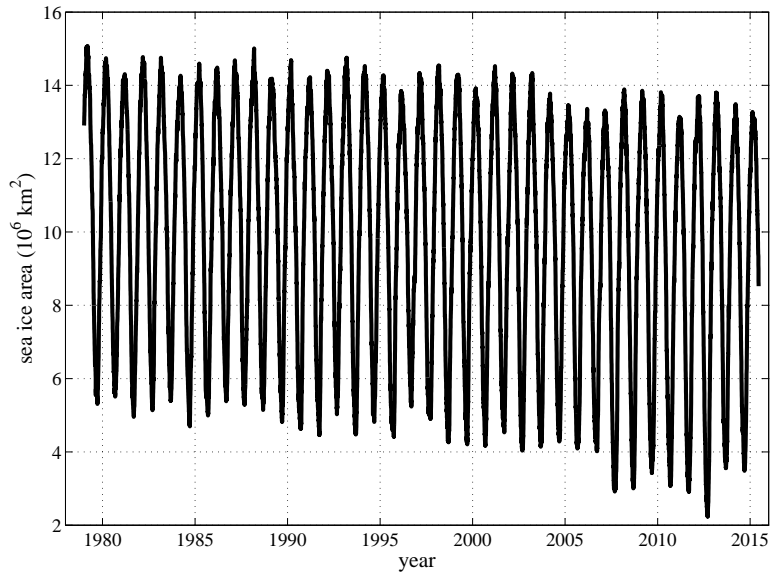


**Figure 9.** Arctic sea ice area satellite observations from 1979 to present day (2015) obtained from The Cryosphere Today project of the University of Illinois.

constant  $D_a$  and a changing time scale. However, the time scales inferred from either the phase lag  
 550 or amplitude are not changing appreciably and therefore it seems unlikely the system is approaching  
 a local bifurcation.

We note that the phase lag is a more robust indicator. This is because the phase lag depends only  
 on the product of the frequency of the forcing and the system time scale whereas the amplitude  
 depends additionally on the amplitude of the driving,  $D_a$ , which may well be changing throughout  
 555 the observational period and could account for some or all of the increase seen in the amplitude in  
 figure 10. Although the solar insolation will be a large component of the forcing amplitude and is  
 essentially fixed, other factors such as clouds as well as air and sea temperatures will also factor  
 into the driving amplitude. Geometrical constraints imposed by land masses affecting the maximal  
 extent of the sea ice will also influence the amplitude of the sea ice oscillation when ice extent is  
 560 large (Eisenman (2010)). In contrast, we can take the frequency of the driving to be essentially fixed  
 by the annual solar insolation cycle making the phase lag more robust.

~~We have also plotted the~~ In the lower panel of figure 10 we have plotted the ratio of the second and  
 third harmonic amplitudes to the amplitude of the fundamental harmonic with time using a sliding  
 window of 10 complete cycles against the year at the end of the window. We have used the minimal  
 window length needed to resolve both harmonics reliably. This indicator also shows no clear trend  
 with time.  
 565

We have also calculated the lag 1 autocorrelation of the return map. From phase lag, the estimate time scale of the sea ice is 0.5 yrs ( $\omega\tau \sim \pi$ ) which is less than  $\tau/T > 1$  needed for a reliable estimate. However, the estimated time scale is uncertain and it is conceivable the return map analysis might work. As there are only 37 complete years of data, any return map time series has a maximum of 37 data points. To discern any trend in the autocorrelation one needs as many windows as possible, however this results in a decreasing number of data points per time series and an increasing error in the estimate. We have therefore chosen a sliding window of 20 cycles although the results are invariant to this choice, always being very uncertain. We linearly detrend the cycle in each sliding window and then create the return map time series from that detrended window. One can also choose at which point in the cycle one wants to take the return map from and this additional freedom is utilized in the right hand panel in figure 12. Lag 1 autocorrelation is plotted against sliding window end year ( $x$  axis) and day of the year in each cycle the return map generated on (the  $y$  axis). We create a new return maps every 10 days giving 36 different points within each cycle. As seen in the figure autocorrelation depends very heavily on where in the cycle one chooses to generate the map, a sign that the return map is not a good approach for this system. A good return map should be largely invariant to where in the cycle it is taken provided the cycle is stable and not changing. In the left hand panel of figure 12 we plot the standard error divided by the autocorrelation. Note that most estimates of lag 1 autocorrelation have standard errors larger than half their value giving very uncertain estimates. In an effort to reduce the uncertainty in the estimate we have also taken the mean autocorrelation over all points in the cycle the return map is taken in figure 13. The mean lag 1 autocorrelation is  $0.16 \pm 0.26$  which corresponds to a (very uncertain) time scale of  $\tau \approx 0.55$  yrs. This is consistent with the estimates from the phase lag. This also suggests that the sampling interval  $T > \tau$  and therefore determining the time scale using the return map approach is difficult. We have increased the sliding window to 37 years to minimize the standard error in the estimate, however one will not be able to then see a trend in autocorrelation. Even so, the standard errors are still greater than half the estimate.

We have also plotted the full spectrum of the ratios  $A_n/A_1$  for the entire time series in figure 11. We note the nonlinear effects are quite prominent in this system, second and third harmonics are around an order of magnitude smaller than the linear response, although we can still probably get away with the linear analysis. Forth, fifth and sixth harmonics are also visible. These nonlinearities may be due to albedo effect or to the geometrical effects of the Arctic ocean basin (Eisenman (2010)).

To conclude, from this simple analysis it seems that the system's time scale and therefore stability is not changing appreciably if at all and it is unlikely to be approaching a local bifurcation. However, simple theoretical models, such as Eisenman and Wettlaufer (2009) ~~and Eisenman (2012)~~, Eisenman (2012) and Bathiany et al. (2016) (who also used a return map approach) suggest that the sea ice time scale does not change very much approaching the bifurcation, even decreasing slightly

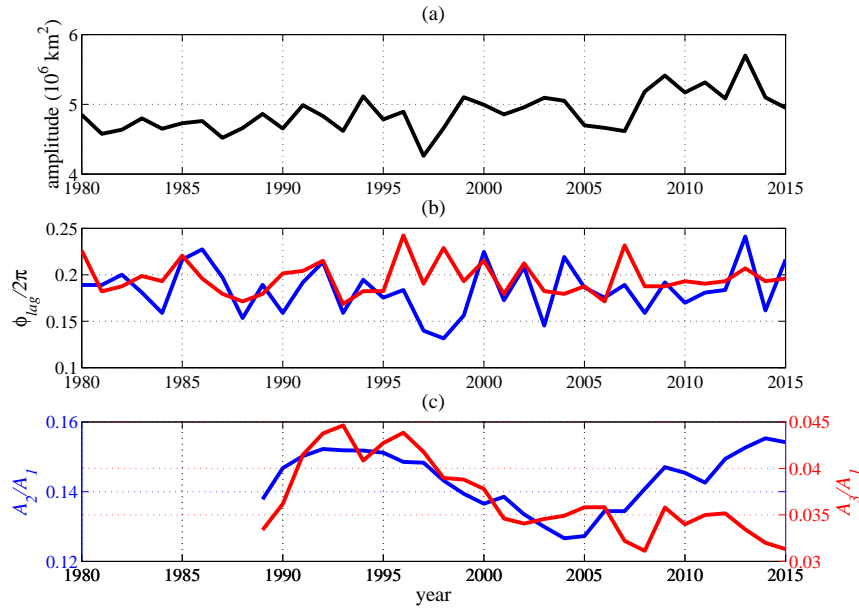


**Figure 10.** In the upper panel amplitude of sea ice area oscillation within each annual cycle is plotted against year and in the lower middle panel phase lag is plotted between the sea ice area minimum (red line) and maximum (blue line) and the solar insolation minimum and maximum respectively against the year. In the lower panel, the 2nd (blue) and 3rd (red) harmonic amplitudes  $A_n/A_1$  are plotted against year end using a sliding window of 10 years. The oscillation amplitude is increasing however the phase lag is not. Harmonic amplitudes also show no convincing trend.

before rapidly changing over a very small interval and therefore would be very hard to detect if present.

## 605 5 Conclusions

Much previous work on detecting local bifurcations from time series required one to be able to partition the universe into widely separated time scales and model the system dynamics as overdamped. When this is the case one can use the usual, statistical fixed point early warning indicators of increasing lag 1 autocorrelation and variance since these indicators measure the system's response to small perturbations away from its fixed point by the fast, noisy processes. It is the response to this small, noisy forcing that allows one to measure the system's time scale. The systems we have been looking at in this paper do not have fast or random forcing. The systems considered here have deterministic forcing with a period roughly that of its time scale although the dynamics are still overdamped. Deterministic forcing again allows one to infer the system's time scale simply by measuring the response to the forcing. ~~We found~~ without the need for large amounts of data required by statistical

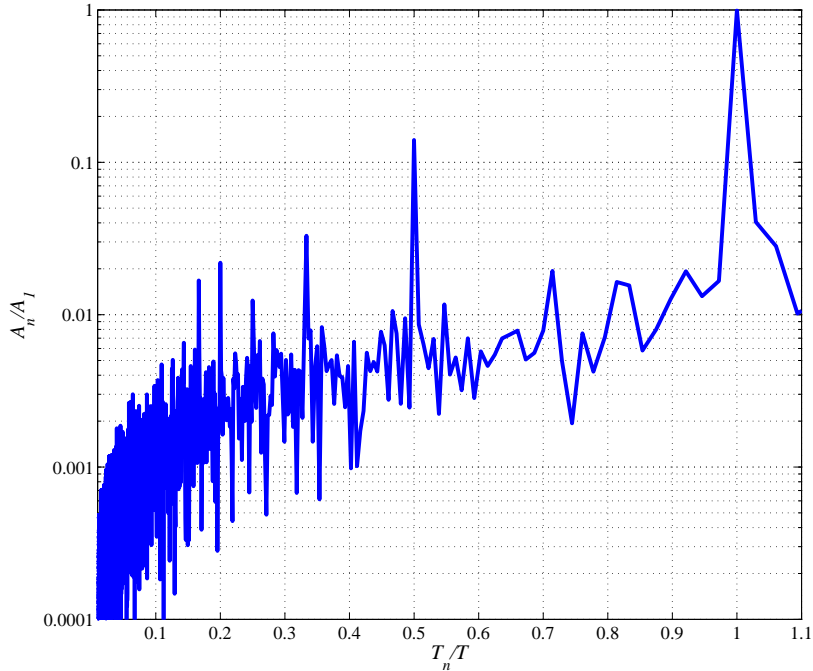


**Figure 11.** Ratio of the  $n$ th order harmonic amplitude to the fundamental harmonic amplitude  $A_n/A_1$  found from the Fourier transform of the Arctic sea ice area time series against the ratio of the  $n$ th harmonic period to the fundamental harmonic period  $T_n/T$ . One can see the Arctic sea ice response features prominent second, third, forth, fifth and sixth harmonics in its spectrum.

quantities for robust estimates. We used two analogous early warning indicators to ~~the lag 1~~ autocorrelation and variance in these systems; these were phase lag and response amplification respectively. Just as autocorrelation is more robust as an indicator (it is a function of fewer parameters), the same is true of phase lag, only depending on the frequency of the forcing and the time scale of the system. The system response amplification also depends on the amplitude of forcing, which in many circumstances is probably difficult to measure.

We also ~~showed that by taking~~ used a Fourier transform of the time series ~~one can to~~ quantify how nonlinear the system is behaving and whether the linear approximations usually made are good. Further, by using a sliding window within the time series, one may also look at the evolution of the harmonic amplitudes as a further early warning indicator.

We ~~applied these new~~ also discussed return map methods that essentially convert a periodic attractor to a fixed point type so that one may use the usual fixed point indicators. We also showed there was a complementarity between return map indicators and phase lag and response amplification, the latter being more useful for regimes in which  $\omega T \sim 1$  and the former being more useful when  $\omega T > 2\pi$ .



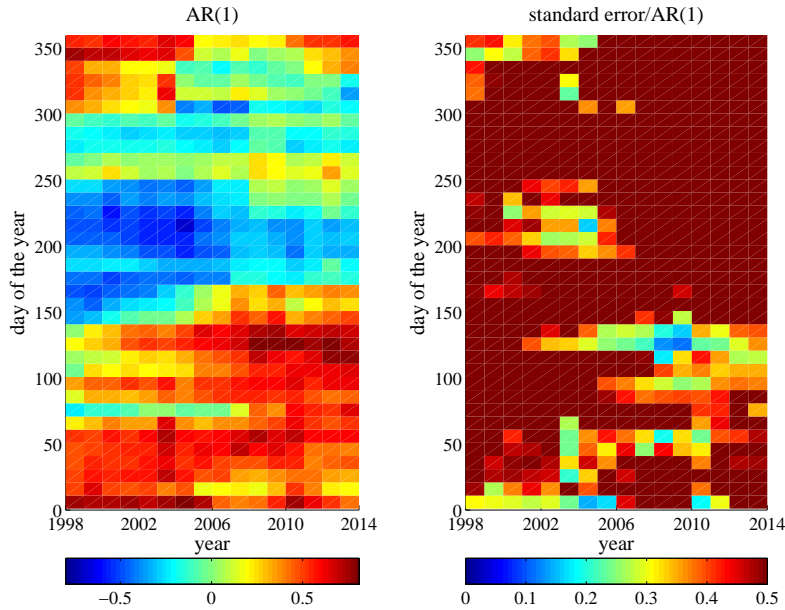


**Figure 12.** Left panel: Lag 1 autocorrelation of the return map against sliding window end year using a sliding window of 20 years ( $x$  axis) and point within the cycle the return map is created on the  $y$  axis (we create return maps every 10 days). One sees autocorrelation depends very heavily on where in the cycle one chooses to generate the the return map. Right panel: Standard error of the autocorrelation return map estimate divided by the estimate against sliding window end year. The estimate is very uncertain almost everywhere with standard errors generally being at least half as big as the estimate.

We applied these indicators to satellite observations of Arctic sea ice area, a system whose period of forcing, effectively the annual cycle of insolation, is similar to the time scale of the system. This is also a system that has been conjectured to have a tipping point due to a local bifurcation. We did not find any detectable critical slowing down and therefore signs of this bifurcation. It should be noted  
 635 however simple models of the sea ice suggest critical slowing down only occurs very close to the bifurcation making it very hard to detect.

**Appendix A: ~~Early warnings~~ Phase lag and response amplification with arbitrary periodic forcing**

~~Here we give the derivation~~ Phase lag and response amplification can be found for the more general  
 640 case of any type of periodic forcing  $D$  ~~.That is we solve the equation by solving~~

$$\dot{x} + \frac{x}{\tau} = D(t) \tag{A1}$$

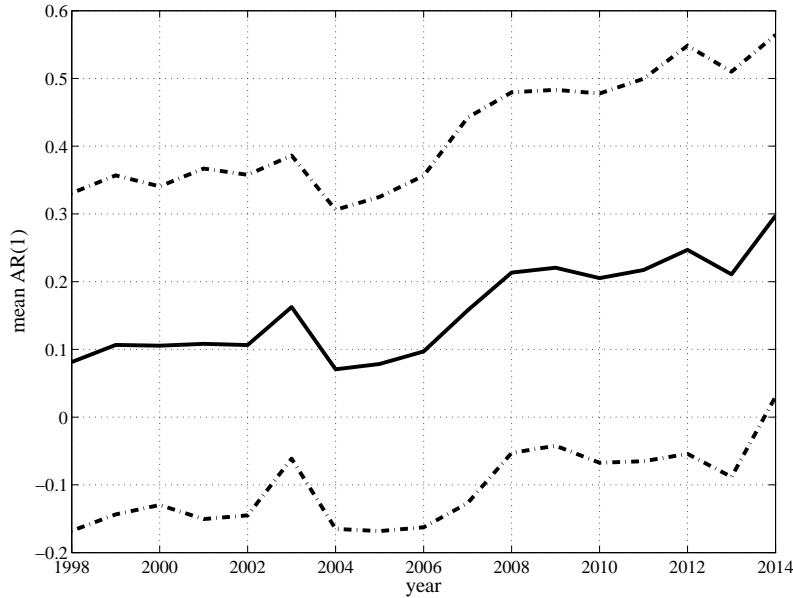


**Figure 13.** Mean lag 1 autocorrelation of the return map across all starting points within the cycle using a sliding window of 20 years. This is the same as figure 12 with the mean taken along the  $y$  axis. Estimated autocorrelation is still very uncertain. The mean is the solid line with the dotted lines being the mean plus/minus the standard error. The mean value across all years  $0.16 \pm 0.26$  which corresponds to a (very uncertain) time scale of  $\tau \approx 0.55$  yrs.

$\tau$  the timescale of the system (the  $e$  folding time). For any periodic forcing,  $D(t)$  with period  $T$  can be written as the Fourier series

$$D(t) = \sum_{i=0}^N B_i \cos(\omega_i t + \chi_i). \quad (\text{A2})$$

645  $B_i$  are the amplitudes of the different component sinusoidal waves,  $\omega_i = \frac{2\pi i}{T}$  are the frequencies of the components and  $\chi_i$  are the phases of each of the components. As the equation is linear the superposition principle holds. That is, we assume the solution has the form

$$x(t) = \sum_{i=0}^N x_i(t) \quad (\text{A3})$$

by setting all but the  $i$ th term of the driving to zero we can solve the  $N + 1$  equations

650  $\dot{x}_i + \frac{x_i}{\tau} = B_i \cos(\omega_i t + \chi_i) \quad (\text{A4})$

for each  $x_i(t)$  ~~which is just the same as the original sinusoidally forced equation. We can then superpose them.~~ These solutions can be superposed to obtain the full solution to any periodic driving

term. ~~The solution of the forced system~~ This is

$$655 \quad x(t) = \sum_{i=0}^N \frac{\tau B_i}{\sqrt{1 + \omega_i^2 \tau^2}} [\cos(\omega_i t + \chi_i - \arctan(\omega_i \tau)) - e^{-\frac{t}{\tau}} \cos(\chi_i - \arctan(\omega_i \tau))] + x_0 e^{-\frac{t}{\tau}} \quad (\text{A5})$$

which settles into orbit

$$x(t) = \sum_{i=0}^N \frac{\tau B_i}{\sqrt{1 + \omega_i^2 \tau^2}} \cos(\omega_i t + \chi_i - \arctan(\omega_i \tau)) \quad (\text{A6})$$

660 when  $t \gg \tau$ , that is, the solution is just the sum of each of the forcing components  $i$ , each with a response amplification of

$$\frac{\tau}{\sqrt{1 + \omega_i^2 \tau^2}} \quad (\text{A7})$$

and a response lagging the forcing with a phase of

$$\phi_i^{lag} = \arctan(\omega_i \tau). \quad (\text{A8})$$

665 One can find out what these phase lags and amplitudes are by taking the Fourier transform of the time series of both the forcing and response.

*Acknowledgements.* ~~he~~ The research leading to these results has received funding from the European Union Seventh Framework Programme FP7/2007-2013 under grant agreement no. 603864 (HELIX). We are ~~also~~ grateful to Peter Ashwin, Peter Cox, Michel Crucifix, Vasilis Dakos, Henk Dijkstra, Jan Sieber, Marten Scheffer and Appy Sluijs for the fruitful discussions over beers and balls.

## 670 References

- Armour, K. C., Eisenman, I., Blanchard-Wrigglesworth, E., McCusker, K. E., and Bitz, C. M.: The reversibility of sea ice loss in a state-of-the-art climate model, *Geophys. Res. Lett.*, 38, L16 705, 2011.
- Bathiany, S., van der Bolt, B., Williamson, M. S., Lenton, T. M., Scheffer, M., van Nes, E., and Notz, D.: Trends in sea-ice variability on the way to an ice-free Arctic, *The Cryosphere Discuss.*, doi:doi:10.5194/tc-2015-209, 675 2016.
- Budyko, M. I.: The effect of solar radiation variations on the climate of the Earth, *Tellus*, 21, 611–619, 1969.
- Carpenter, S., Cole, J., Pace, M. L., Batt, R., Brock, W. A., Cline, T., Coloso, J., Hodgson, J. R., Kitchell, J. F., Seekell, D. A., Smith, L., and Weidel, B.: Early Warnings of Regime Shifts: A Whole-Ecosystem Experiment, *Science*, 332, 1079–1082, 2011.
- 680 Crucifix, M.: Oscillators and relaxation phenomena in Pleistocene climate theory, *Phil. Trans. R. Soc. A*, 370, 1140–1165, 2012.
- Crucifix, M.: Why could ice ages be unpredictable?, *Clim. Past*, 9, 2253–2267, 2013.
- Dakos, V., Scheffer, M., van Nes, E. H., Brovkin, V., Petoukhov, V., and Held, H.: Slowing down as an early warning signal for abrupt climate change, *P. Natl. Acad. Sci. USA*, 105, 14 308–14 312, 2008.
- 685 Domb, C., Green, M. S., and Lebowitz, J., eds.: *Phase transitions and critical phenomena*, vol. 1-20, Academic Press, 1972-2001.
- Eisenman, I.: Geographic muting of changes in the Arctic sea ice cover, *Geophys. Res. Lett.*, 37, L16 501, 2010.
- Eisenman, I.: Factors controlling the bifurcation structure of sea ice retreat, *J. Geophys. Res.*, 117, D01 111, 2012.
- 690 Eisenman, I. and Wettlaufer, J. S.: Nonlinear threshold behaviour during the loss of Arctic sea ice, *P. Natl. Acad. Sci. USA*, 106, 28–32, 2009.
- Gammaitoni, L., Hänggi, P., Jung, P., and Marchesoni, F.: Stochastic resonance, *Rev. Mod. Phys.*, 70, 223–287, 1998.
- Held, H. and Kleinen, T.: Detection of climate system bifurcations by degenerate fingerprinting, *Geophys. Res. Lett.*, 31, L23 207, 2004.
- 695 Jung, P. and Hänggi, P.: Hopping and phase shifts in noisy periodically driven bistable systems, *Z. Phys. B*, 90, 255–260, 1993.
- Kuznetsov, Y. A.: *Elements of Applied Bifurcation Theory*, third edition, Springer, 2004.
- Lenton, T. M.: Early warning of climate tipping points, *Nature Climate Change*, 1, 201–209, 2011.
- 700 Lindsay, R. W. and Zhang, J.: The thinning of the Arctic sea ice, 1988-2003: Have we passed a tipping point?, *J. Clim.*, 18, 4879–4894, 2005.
- Livina, V. N. and Lenton, T. M.: A recent tipping point in the Arctic sea-ice cover: abrupt and persistent increase in the seasonal cycle since 2007, *Cryosphere*, 7, 275–286, 2013.
- Main, I. G.: *Vibrations and Waves*, Cambridge University Press, 3rd edn., 1993.
- 705 McNamara, B. and Wiesenfeld, K.: Theory of stochastic resonance, *Phys. Rev. A*, 39, 4854–4869, 1989.
- Ridley, J. K., Lowe, J. A., and Hewitt, H. T.: How reversible is sea-ice loss?, *Cryosphere*, 6, 193–198, 2012.
- Saedeleer, B. D., Crucifix, M., and Wiczorek, S.: Is the astronomical forcing a reliable and unique pacemaker for climate? A conceptual model study, *Clim. Dyn.*, 40, 273–294, 2013.

- 710 Saltzman, B.: Dynamical Paleoclimatology: Generalized theory of global climate change, Academic Press,  
2002.
- Scheffer, M., Bacompte, J., Brock, W. A., Brovkin, V., Carpenter, S. R., Dakos, V., Held, H., van Nes, E. H.,  
Rietkerk, M., and Sugihara, G.: Early warning signals for critical transitions, *Nature*, 461, 53–59, 2009.
- 715 Scheffer, M., Carpenter, S. R., Lenton, T. M., Bascompte, J., Brock, W., Dakos, V., van de Koppel, J., van de  
Leemput, I. A., Levin, S. A., van Nes, E. H., Pascual, M., and Vandermeer, J.: Anticipating Critical Transi-  
tions, *Science*, 338, 344–348, 2012.
- Sellers, W. D.: A global climate model based on the energy balance of the Earth-atmosphere system, *J. Appl.  
Meteorol.*, 8, 392–400, 1969.
- Shneidman, V. A., Jung, P., and Hänggi, P.: Power spectrum of a driven bistable system, *Europhys. Lett.*, 26,  
571–576, 1994.
- 720 Strogatz, S. H.: *Nonlinear Dynamics and Chaos*, Westview Press, 2001.
- Thompson, J. M. T. and Sieber, J.: Predicting climate tipping as a noisy bifurcation: A review, *Int. J. Bif. Chaos*,  
21, 399–423, 2011.
- Thompson, J. M. T. and Stewart, H. B.: *Nonlinear Dynamics and Chaos*, second edition, John Wiley and Sons,  
Ltd., 2002.
- 725 Wang, M. and Overland, J. E.: A sea ice free summer Arctic within 30 years: An update from CMIP5 models,  
*Geophys. Res. Lett.*, 39, L18 501, 2012.
- Wiesenfeld, K.: Noisy precursors of nonlinear instabilities, *J. Stat. Phys.*, 38, 1071–1097, 1985.
- Wiesenfeld, K. and McNamara, B.: Small-signal amplification in bifurcating dynamical systems, *Phys. Rev. A*,  
33, 629–641, 1986.
- 730 Williamson, M. S. and Lenton, T. M.: Detection of bifurcations in noisy coupled systems from multiple time  
series, *Chaos*, 25, 036 407, 2015.